Global inorganic nitrate production mechanisms: Comparison of a global model with nitrate isotope observations

Becky Alexander[1], Tomás Sherwen[2,3], Christopher D. Holmes[4], Jenny A. Fisher[5], Qianjie Chen[1,6], Mat J. Evans[2,3], Prasad Kasibhatla[7]

[1]Department of Atmospheric Sciences, University of Washington, Seattle, WA 98195, USA

[2]Wolfson Atmospheric Chemistry Laboratories, Department of Chemistry, University of York, York YO10 5DD, UK

[3]National Center for Atmospheric Science, University of York, York YO10 5DD, UK

[4]Department of Earth, Ocean and Atmospheric Science, Florida State University, Tallahassee, FL 32306, USA

[5]Centre for Atmospheric Chemistry, University of Wollongong, Wollongong, New South Wales 2522, Australia

[6]Now at Department of Chemistry, University of Michigan, Ann Arbor, MI 48109, USA

[7]Nicholas School of the Environment, Duke University, Durham, NC 27708, USA

Correspondence to: Becky Alexander (beckya@uw.edu)

Abstract. The formation of inorganic nitrate is the main sink for nitrogen oxides ($NO_x = NO + NO_2$). Due to the importance of NO_x for the formation of tropospheric oxidants such as the hydroxyl radical (OH) and ozone, understanding the mechanisms and rates of nitrate formation is paramount for our ability to predict the atmospheric lifetimes of most reduced trace gases in the atmosphere. The oxygen isotopic composition of nitrate ($\Delta^{17}O(nitrate)$) is determined by the relative importance of NO_x sinks, and thus can provide an observational constraint for NO_x chemistry. Until recently, the ability to utilize $\Delta^{17}O(nitrate)$ observations for this purpose was hindered by our lack of knowledge about the oxygen isotopic composition of ozone ($\Delta^{17}O(O_3)$). Recent and spatially widespread observations of $\Delta^{17}O(O_3)$, and motivate an updated comparison of modeled and observed $\Delta^{17}O(nitrate)$ and a

reassessment of modeled nitrate formation pathways. Model updates based on recent laboratory studies of heterogeneous reactions renders dinitrogen pentoxide (N_2O_5) hydrolysis as important as NO_2 + OH (both 41%) for global inorganic nitrate production near the surface (below 1 km altitude). All other nitrate production mechanisms individually represent less than 6% of global nitrate production near the surface, but can be dominant locally. Updated reaction rates for aerosol uptake of NO_2 result in significant reduction of nitrate and nitrous acid (HONO) formed through this pathway in the model, and render NO_2 hydrolysis a negligible pathway for nitrate formation globally. Although photolysis of aerosol nitrate may have implications for NO_x, HONO and oxidant abundances, it does not significantly impact the relative importance of nitrate formation pathways. Modeled $\Delta^{17}O$(nitrate) (28.6 ± 4.5‰) compares well with the average of a global compilation of observations (27.6 ± 5.0‰) when assuming $\Delta^{17}O(O_3)$ = 26‰, giving confidence in the model's representation of the relative importance of ozone versus HO_x (= OH + HO_2 + RO_2) in NO_x cycling and nitrate formation on the global scale.

1. Introduction

Nitrogen oxides (NO_x = NO + NO_2) are a critical ingredient for the formation of tropospheric ozone (O_3). Tropospheric ozone is a greenhouse gas, is a major precursor for the hydroxyl radical (OH), and is considered an air pollutant due to its negative impacts on human health. The atmospheric lifetime of NO_x is determined by its oxidation to inorganic and organic nitrate. The formation of inorganic nitrate (HNO_3(g) and particulate NO_3^-) is the dominant sink for NO_x globally, while formation of organic nitrate may be significant in rural and remote continental locations (Browne and Cohen, 2014). Organic nitrate as a sink for NO_x may be becoming more important in regions in North America and Europe where NO_x emissions have declined (Zare et al., 2018). Uncertainties in the rate of oxidation of NO_x to nitrate has been shown to represent a significant source of uncertainty for ozone and OH formation in models (e.g., Newsome and Evans (2017)) , with implications for our understanding of the atmospheric lifetime of species such as methane, whose main sink is reaction with OH.

NO_x is emitted to the atmosphere primarily as NO by fossil fuel and biomass/biofuel burning, soil microbes, and lightning. Anthropogenic sources from fossil fuel and biofuel burning and from the application of fertilizers to soil for agriculture currently dominate NO_x sources to the atmosphere (Jaeglé et al., 2005). After emission, NO is rapidly

1   oxidized to NO_2 by ozone (O_3), peroxy (HO_2) and hydroperoxy radicals (RO_2), and halogen oxides (e.g., BrO). During

2   the daytime, NO_2 is rapidly photolyzed to NO + O at wavelengths (λ) < 398 nm. NO_x cycling between NO and NO_2

3   proceeds several orders of magnitude faster than oxidation of NO_x to nitrate during the daytime (Michalski et al.,

4   2003).

6   Formation of inorganic nitrate is dominated by oxidation of NO_2 by OH during the day and by the hydrolysis of

7   dinitrogen pentoxide (N_2O_5) at night (Alexander et al., 2009). Recent implementation of reactive halogen chemistry

8   in models of tropospheric chemistry show that formation of nitrate from the hydrolysis of halogen nitrates (XNO_3,

9   where X = Br, Cl, or I) is also a sink for NO_x with implications for tropospheric ozone, OH, reactive halogens, and

10   aerosol formation (Schmidt et al., 2016;Sherwen et al., 2016;Saiz-Lopez et al., 2012;Long et al., 2014;Parrella et al.,

11   2012;von Glasow and Crutzen, 2004;Yang et al., 2005). Other inorganic nitrate formation pathways include

12   hydrogen-abstraction of hydrocarbons by the nitrate radical (NO_3), heterogeneous reaction of N_2O_5 with particulate

13   chloride (Cl^-), heterogeneous uptake of NO_2 and NO_3, direct oxidation of NO to HNO_3 by HO_2, and hydrolysis of

14   organic nitrate (Atkinson, 2000). Inorganic nitrate partitions between the gas ($HNO_3(g)$) and particle (NO_3^-) phases,

15   with its relative partitioning dependent upon aerosol abundance, aerosol liquid water content, aerosol chemical

16   composition, and temperature. Inorganic nitrate is lost from the atmosphere through wet or dry deposition to the

17   Earth's surface with a global lifetime against deposition on the order of 3-4 days (Park et al., 2004).

19   Formation of inorganic nitrate was thought to be a permanent sink for NO_x in the troposphere due to the slow

20   photolysis of nitrate compared to deposition. However, laboratory and field studies have shown that NO_3^- adsorbed

21   on surfaces is photolyzed at rates much higher than $HNO_3(g)$ (Ye et al., 2016). For example, the photolysis of NO_3^-

22   in snow grains on ice sheets has a profound impact on the oxidizing capacity of the polar atmosphere (Domine and

23   Shepson, 2002). More recently, observations of NO_x and nitrous acid (HONO) provide evidence of photolysis of

24   aerosol NO_3^- in the marine (Reed et al., 2017;Ye et al., 2016) and continental (Ye et al., 2018;Chen et al., 2019)

25   boundary layer, with implications for ozone and OH (Kasibhatla et al., 2018).

27   Organic nitrates form during reaction of NO_x and NO_3 with biogenic volatile organic compounds (BVOCs) and their

28   oxidation products (organic peroxy radicals, RO_2) (Browne and Cohen, 2014;Liang et al., 1998). Products of these

reactions include peroxy nitrates (RO_2NO_2) and alkyl and multifunctional nitrates ($RONO_2$) (O'Brien et al., 1995). Peroxy nitrates are thermally unstable and decompose back to NO_x on the order of minutes to days at warm temperatures. Decomposition of longer-lived peroxy nitrates such as peroxyacetyl nitrate (PAN) can provide a source of NO_x to remote environments (Singh et al., 1992). The fate of $RONO_2$ is uncertain. First-generation $RONO_2$ is oxidized to form second-generation $RONO_2$ species with a lifetime of about a week for the first-generation species with ≥ 4 carbon atoms, and up to several weeks for species with fewer carbon atoms (e.g., days to weeks for methyl nitrate) (Fisher et al., 2018). Subsequent photolysis and oxidation of second-generation $RONO_2$ species can lead to the recycling of NO_x (Müller et al., 2014), although recycling efficiencies are highly uncertain (Horowitz et al., 2007;Paulot et al., 2009). $RONO_2$ can also partition to the particle phase ($pRONO_2$) contributing to organic aerosol formation (Xu et al., 2015). $pRONO_2$ is removed from the atmosphere by deposition to the surface, or through hydrolysis to form inorganic nitrate and alcohols (Rindelaub et al., 2015;Jacobs et al., 2014).

The oxygen isotopic composition ($\Delta^{17}O = \delta^{17}O - 0.52 \times \delta^{18}O$) of nitrate is determined by the relative importance of oxidants leading to nitrate formation from the oxidation of NO_x (Michalski et al., 2003). Observations of the oxygen isotopic composition of nitrate ($\Delta^{17}O(nitrate)$) have been used to quantify the relative importance of different nitrate formation pathways and to assess model representation of the chemistry of nitrate formation in the present day (Alexander et al., 2009;Michalski et al., 2003;Costa et al., 2011;Ishino et al., 2017a;Morin et al., 2009;Morin et al., 2008;Savarino et al., 2007;Kunasek et al., 2008;Savarino et al., 2013;McCabe et al., 2007;Morin et al., 2007;Hastings et al., 2003;Kaiser et al., 2007;Brothers et al., 2008;Ewing et al., 2007) and in the past from nitrate archived in ice cores (Sofen et al., 2014;Alexander et al., 2004;Geng et al., 2014;Geng et al., 2017). Ozone-influenced reactions in NO_x oxidation lead to high $\Delta^{17}O(nitrate)$ values while HO_x-influenced reactions lead to $\Delta^{17}O(nitrate)$ near zero. Oxidation by XO (where X = Br, Cl, or I) leads to $\Delta^{17}O(nitrate)$ values similar to reactions with ozone because the oxygen atom in XO is derived from the reaction $X + O_3$. Therefore, $\Delta^{17}O(nitrate)$ is determined by the relative importance of $O_3 + XO$ versus HO_x (= $OH + HO_2 + RO_2$) in both NO_x cycling and oxidation to nitrate. Although freshly emitted NO will have $\Delta^{17}O(NO) = 0‰$, NO_x achieves isotopic equilibrium during the daytime due to rapid NO_x cycling, so that its $\Delta^{17}O$ value ($\Delta^{17}O(NO_x)$) is solely determined by the relative abundance of ($O_3 + XO$) to ($HO_2 + RO_2$) (Michalski et al., 2003).

1   The $\Delta^{17}O$ value of HO_x ($\Delta^{17}O(HO_x)$) is near zero due to isotopic exchange of OH with water vapor (Dubey et al.,

2   1997).   Previously, observations of the $\Delta^{17}O$ value of ozone ($\Delta^{17}O(O_3)$) showed a large range (6 – 54‰) (Johnston

3   and Thiemens, 1997;Krankowsky et al., 1995), in contrast to laboratory and modeling studies suggesting that the range

4   of $\Delta^{17}O(O_3)$ in the troposphere should be relatively narrow (30-46 ‰) (Morton et al., 1990;Thiemens, 1990). The

5   large range of observed $\Delta^{17}O(O_3)$ values is thought to be due to sampling artifacts (Brenninkmeijer et al., 2003).

6   Uncertainty in the value of $\Delta^{17}O(O_3)$ has been the largest source of uncertainty in quantification of nitrate formation

7   pathways using observations of $\Delta^{17}O$(nitrate) (Alexander et al., 2009). Previous modeling studies showed good

8   agreement with observations of $\Delta^{17}O$(nitrate) when assuming that the bulk oxygen isotopic composition of ozone

9   ($\Delta^{17}O(O_3)$) is equal to 35‰ (Alexander et al., 2009;Michalski et al., 2003); but varied in their assumption on terminal

10   oxygen atom versus statistical isotopic transfer from O_3 to the reactant (NO and NO_2). This is an important distinction

11   because it is now known that the ^{17}O enrichment in O_3 is contained entirely in its terminal oxygen atoms, and it is the

12   terminal oxygen atom that is transferred from O_3 (Vicars et al., 2012;Berhanu et al., 2012;Bhattacharya et al.,

13   2008;Savarino et al., 2008;Michalski and Bhattacharya, 2009;Bhattacharya et al., 2014), so that the $\Delta^{17}O$ value of the

14   oxygen atom transferred from ozone to the product is 50% larger than the bulk $\Delta^{17}O(O_3)$ value. Recently, much more

15   extensive observations of $\Delta^{17}O(O_3)$ using a new technique (Vicars et al., 2012) consistently show $\Delta^{17}O(O_3) = 26 \pm$

16   1‰ in diverse locations (Vicars et al., 2012;Ishino et al., 2017b;Vicars and Savarino, 2014), and suggest that previous

17   modeling studies are biased low in $\Delta^{17}O$(nitrate) (e.g., Alexander et al. (2009)), which would occur if the model

18   underestimated the relative role of ozone in NO_x chemistry. These new observations of $\Delta^{17}O(O_3)$, combined with

19   improved understanding and hence more comprehensive chemical representation of nitrate formation in models,

20   motivates an updated comparison of observed and modeled $\Delta^{17}O$(nitrate) as an observational constraint for the relative

21   importance of nitrate formation pathways in the atmosphere. Note that laboratory studies show that the magnitude of

22     $\Delta^{17}O(O_3)$ is dependent on temperature and pressure (Heidenreich and Thiemens, 1986;Thiemens, 1990;Morton et al.,

23   1990). The observations of $\Delta^{17}O(O_3)$ by Vicars et al. (2012, 2013) were at the surface over a large temperature range,

24   but may not reflect the value of $\Delta^{17}O(O_3)$ at higher altitudes. However, with the exception of lightning, whose

25   emissions are presently several times smaller than NO_x emissions from anthropogenic and biomass burning sources

26   (Murray, 2016), NO_x sources emit at the surface. With a NO_x lifetime relative to its conversion to nitrate on the order

27   of one day (Levy et al., 1999), most nitrate formation also occurs near the surface. Here, we examine the relative

1 contribution of each nitrate formation pathway in a global chemical transport model and compare the model with

2 surface observations of $\Delta^{17}O$(nitrate) from around the world.

4 **2. Methods**

6 We use the GEOS-Chem global chemical transport model version 12.0.0 driven by assimilated meteorology from the

7 MERRA-2 reanalysis product with a native resolution of 0.5° x 0.625° and 72 vertical levels from the surface up to

8 the 0.01 hPa pressure level. For computational expediency, the horizontal and vertical resolution were downgraded

9 to 4° x 5° and 47 vertical levels.   GEOS-Chem was originally described in Bey et al. (2001) and includes coupled

10 HO_x-NO_x-VOC-ozone-halogen-aerosol tropospheric chemistry as described in Sherwen et al. (2016) and Sherwen et

11 al. (2017) and organic nitrate chemistry as described in Fisher et al. (2016). Aerosols interact with gas-phase chemistry

12 through the effect of aerosol extinction on photolysis rates (Martin et al., 2003) and heterogeneous chemistry (Jacob,

13 2000). The model calculates deposition for both gas species and aerosols (Liu et al., 2001;Zhang et al., 2001;Wang

14 et al., 1998).

16 Global anthropogenic emissions, including NO_x, are from the Community Emissions Data System (CEDS) inventory

17 from 1950 – 2014 C.E. (Hoesly et al., 2018a). The CEDS global emissions inventory is overwritten by regional

18 anthropogenic emissions inventories in the U.S. (EPA/NE11), Canada (CAC), Europe (EMEP), and Asia (MIX (Li et

19 al., 2017)). Global shipping emissions are from the International Comprehensive Ocean-Atmosphere Data Set

20 (ICOADS), which was implemented into GEOS-Chem as described in Lee et al. (2011). NO_x emissions from ships

21 are processed using the PARANOX module described in Vinken et al. (2011) and Holmes et al. (2014) to account for

22 non-linear, in-plume ozone and HNO_3 production. Lightning NO_x emissions match the OTD/LIS satellite

23 climatological observations of lightning flashes as described by Murray et al. (2012). Emissions from open fires are

24 from the Global Fire Emissions Database (GFED4.1). Biogenic soil NO_x emissions are described in Hudman et al.

25 (2012). Aircraft emissions are from the Aviation Emissions Inventory Code (AEIC) (Stettler et al., 2011).

27 Chemical processes leading to nitrate formation in GEOS-Chem have expanded since the previous work of Alexander

28 et al. (2009). Figure 1 summarizes the formation of inorganic nitrate in the current model. In the model, NO is

1   oxidized by O_3, HO_2, RO_2 and halogen oxides (XO = BrO, ClO, IO, and OIO) to form NO_2. The reaction of NO +

2   HO_2 can also form HNO_3 directly, although the branching ratio for this pathway is < 1% (Butkovskaya et al., 2005).

3   NO_2 can form HNO_3 directly from its reaction with OH and through hydrolysis on aerosol surfaces. NO_2 can react

4   with XO to form halogen nitrates ($BrNO_3$, $ClNO_3$, and INO_3), which can then form HNO_3 upon hydrolysis (as

5   described in Sherwen et al. (2016)). NO_2 can also react with O_3 to form NO_3, which can then react with NO_2,

6   hydrocarbons (HC), and the biogenic VOCs monoterpenes (MTN) and isoprene (ISOP). Reaction of NO_3 with NO_2

7   forms N_2O_5, which can subsequently hydrolyze or react with Cl^- in aerosol to form HNO_3. Reaction of NO_3 with HC

8   forms HNO_3 via hydrogen abstraction. Reactions of NO_3 are only important at night due to its short lifetime against

9   photolysis. Formation of organic nitrate ($RONO_2$) was recently updated in the model as described in Fisher et al.

10   (2016). Reaction of NO_3 with MTN and ISOP can form $RONO_2$. $RONO_2$ also forms from the reaction of NO with

11   RO_2 derived from OH oxidation of BVOCs. $RONO_2$ hydrolyzes to form HNO_3 on a timescale of 1 hour. Inorganic

12   nitrate partitions between the gas ($HNO_3(g)$) and particle (NO_3^-) phase according to local thermodynamic equilibrium

13   as calculated in the ISORROPIA-II aerosol thermodynamic module (Fountoukis and Nenes, 2007). $HNO_3(g)$ and

14   NO_3^- are mainly lost from the atmosphere via wet and dry deposition to the surface.

16   In the "standard" model, hydrolysis of N_2O_5, NO_3 ($\gamma_{NO3} = 1 \times 10^{-3}$), and NO_2 ($\gamma_{NO2} = 1 \times 10^{-4}$) occur on aerosol surfaces

17   only. Uptake and hydrolysis of N_2O_5 on aerosol surfaces depends on the chemical composition of aerosols,

18   temperature, and humidity as described in Evans and Jacob (2005). Recently, Holmes et al. (2019) updated the

19   reaction probabilities of the NO_2 and NO_3 heterogeneous reactions in the model to depend on aerosol chemical

20   composition and relative humidity. Holmes et al. (2019) also updated the N_2O_5 reaction probability to additionally

21   depend on the H_2O and NO_3^- concentrations in aerosol (Bertram and Thornton, 2009). In addition to these updates

22   for hydrolysis on aerosol, Holmes et al. (2019) included the uptake and hydrolysis of N_2O_5, NO_2, and NO_3 in cloud

23   water and ice limited by cloud entrainment rates. We incorporate these updates from Holmes et al. (2019) into the

24   "cloud chemistry" model to examine the impacts on global nitrate production mechanisms. We consider the "cloud

25   chemistry" model as state-of-the science, and as such we focus on the results of this particular simulation. Additional

26   model sensitivity studies are also performed and examined relative to the "standard" model simulation, which

27   represents a more common representation of nitrate chemistry in atmospheric chemistry models. These additional

28   sensitivity simulations are described in Section 4.

2 $\Delta^{17}O$(nitrate) is calculated in the model using monthly-mean, local chemical production rates, rather than by treating

3 different isotopic combinations of nitrate as separate tracers that can be transported in the model. Alexander et al.

4 (2009) transported four nitrate tracers, one each for nitrate production by NO_2+OH, N_2O_5 hydrolysis, NO_3+HC, and

5 nitrate originating from its formation in the stratosphere. Since $\Delta^{17}O(NO_x)$ was not transported in the Alexander et al.

6 (2009) model, it was calculated using local production rates, so effectively only one-third of the $\Delta^{17}O$(nitrate) was

7 transported in Alexander et al. (2009). Accurately accounting for transport of $\Delta^{17}O$(nitrate) in the model would require

8 transporting all individual isotopic combinations of the primary reactant (NO), the final product (nitrate), and each

9 reaction intermediate (e.g., N_2O_5), which we do not do here due to the large computational costs. Thus, the model

10 results shown here represent $\Delta^{17}O$(nitrate) from local NO_x cycling and nitrate production. This may lead to model

11 biases, particularly in remote regions such as polar-regions in winter-time when most nitrate is likely transported from

12 lower latitudes or the stratosphere. This should make less difference in polluted regions where most nitrate is formed

13 locally, or for example in polar regions in summer when photochemical recycling of nitrate in the snowpack represents

14 a significant local source of NO_x at the surface (Domine and Shepson, 2002). Although lack of transport of the isotope

15 tracers adds uncertainty to direct comparison of the model with observations at any particular location, this approach

16 will reflect the full range of possible modeled $\Delta^{17}O$(nitrate) values for the current chemical mechanism, which can

17 then be compared to the range of observed $\Delta^{17}O$(nitrate) values around the globe.

19 The $\Delta^{17}O$(nitrate) value of nitrate produced from each production pathway is calculated as shown in Table 1. The

20 value of A in Table 1 represents the relative importance of the oxidation pathways of NO to NO_2 where the oxygen

21 atom transferred comes from ozone ($NO + O_3$ and $NO + XO$):

22 $$A = \frac{k_{O_3+NO}[O_3] + k_{XO+NO}[XO]}{k_{O_3+NO}[O_3] + k_{XO+NO}[XO] + k_{HO_2+NO}[HO_2] + k_{RO_2+NO}[RO_2]}$$ (E1)

23 In E1, k represents the local reaction rate constant for each of the four reactions, XO = BrO, ClO, IO, and OIO, and

24 we assume $\Delta^{17}O(XO)$ is equal to the $\Delta^{17}O$ value of the terminal oxygen atoms of ozone, as described in more detail

25 below. This effectively assumes that the other oxidation pathways ($NO + HO_2$ and $NO + RO_2$) yield $\Delta^{17}O(NO_x) =$

26 0‰. Although HO_2 may have a small ^{17}O enrichment on the order of 1-2‰ (Savarino and Thiemens, 1999b), the

27 assumption that this pathway yields $\Delta^{17}O(NO_x) = 0$‰ simplifies the calculation and leads to negligible differences in

1 calculated $\Delta^{17}O$(nitrate) (Michalski et al., 2003). This approach assumes that NO_x cycling is in photochemical steady-

2 state, which only occurs during the daytime. *A* is calculated in the model as the 24-hour average NO_2 production rate,

3 rather than the daytime average only. As was shown in Alexander et al. (2009), rapid daytime NO_x cycling dominates

4 the calculated 24-hour averaged *A* value, leading to negligible differences in calculated $\Delta^{17}O$(nitrate) for 24-hour

5 averaged values versus daytime averaged values.

7 NO_x formed during the day will retain its daytime $\Delta^{17}O(NO_x)$ signature throughout the night due to lack of NO_2

8 photolysis (Morin et al., 2011), suggesting similar *A* values for the nighttime reactions (R2, R4, R5, R8, and R10 in

9 Table 1). However, NO emitted at night will not undergo photochemical recycling; initially suggesting that NO will

10 retain its emitted $\Delta^{17}O(NO)$ value of 0‰ prior to sunrise.   Thus, any NO emitted at night and oxidized to NO_2 before

11 sunrise will result in $\Delta^{17}O(NO_2)$ equal to one-half of the $\Delta^{17}O$ value of the oxidant, since only one of the two oxygen

12 atoms of NO_2 will originate from the oxidant. Since HO_x abundance is low at night, ozone will be the dominant

13 oxidant. Thus, NO both emitted and oxidized to NO_2 at night will lead to $A_{night} = 0.5$ (half of the O atoms of NO_2

14 originate from O_3). Although isotopic exchange between NO + NO_2 (Sharma et al., 1970) and NO_2 and NO_3 via

15 thermal dissociation of N_2O_5 (Connell and Johnston, 1979) will tend to increase $\Delta^{17}O(NO)$ above its emitted value of

16 0‰, the bulk $\Delta^{17}O$ value of NO_x plus NO_3 system will be lower at night than during the daytime due to the absence

17 of photochemical cycling at night (Michalski et al., 2014;Morin et al., 2011). Since the atmospheric lifetime of NO_x

18 near the surface against nighttime oxidation to nitrate (R2+R4+R5) is typically greater than 24 hours (Figure S1),

19 most nitrate formed during the nighttime will form from NO_x that reached photochemical equilibrium during the

20 previous day. Thus, we use values of *A* calculated as the 24-hour average NO_2 production rate for calculating the

21 $\Delta^{17}O$(nitrate) value of all nitrate production pathways, including those that can occur at night. Using 24-hour averaged

22 *A* values may lead to an overestimate of $\Delta^{17}O$(nitrate) in locations with more rapid nighttime nitrate formation rates

23 such as in China and India (Figure S1). However, even in these locations the lifetime of NO_x against nighttime

24 oxidation is greater than 12 hours, suggesting that over half of nitrate formation at night occurs from the oxidation of

25 NO_x that reached photochemical equilibrium during the daytime. When comparing modeled $\Delta^{17}O$(nitrate) with

26 observations, we add error bars to model values in these locations (Beijing and Mt. Lulin, Taiwan) that reflect the

27 range of possible *A* values for nighttime nitrate formation, with the high end (A_{high}) reflecting 24-hour average *A* values

1   and the low end assuming that half of nitrate formation occurs from oxidation of NO_x that reached photochemical

2   equilibrium during the daytime ($A_{low} = 0.5A + 0.5A_{night}$, where $A_{night} = 0.5$).

4    $\Delta^{17}O$(nitrate) for total nitrate is calculated in the model according to:

5    $\Delta^{17}O(nitrate) = \sum_{R=R1}^{R10} f_R \Delta^{17}O(nitrate)_R$ (E2)

6   where f_R represents the fractional importance of each nitrate production pathway (R1-R10 in Table 1) relative to total

7   nitrate production, and $\Delta^{17}O$(nitrate)$_R$ is the $\Delta^{17}O$(nitrate) value for each reaction as described in Table 1. To calculate

8    $\Delta^{17}O$(nitrate), we assume that the mean $\Delta^{17}O$ value of the ozone molecule ($\Delta^{17}O(O_3)$) is equal to 26‰ based on recent

9   observations (Vicars et al., 2012;Ishino et al., 2017b;Vicars and Savarino, 2014) , and that it is the terminal oxygen

10   atom that are transferred to the oxidation product during chemical reactions (Savarino et al., 2008;Berhanu et al.,

11   2012). Thus, we assume that the $\Delta^{17}O$ value of the oxygen atom transferred from O_3 ($\Delta^{17}O(O_3^*)$) = 1.5 x $\Delta^{17}O(O_3)$,

12   as in previous work (e.g., (Morin et al., 2011)), where $\Delta^{17}O(O_3^*)$ represents the $\Delta^{17}O$ value of the terminal oxygen

13   atoms in ozone. Assuming that $\Delta^{17}O(O_3)$ = 26‰ based on recent observations, this leads to $\Delta^{17}O(O_3^*)$ = 39‰.

16   **3.   Results and Discussion**

18   Figure 1 shows the relative importance of the different oxidation pathways of NO to NO_2 and nitrate formation below

19   1 km altitude in the model for the "cloud chemistry" simulation, with equivalent values for the "standard" simulation

20   shown in parentheses. We focus on model results near the surface (below 1 km) because these can be compared to

21   observations; currently only surface observations of $\Delta^{17}O$(nitrate) are available. We note that two observation data

22   sets (from Bermuda (Hastings et al., 2003) and Princeton, NJ (Kaiser et al., 2007)) are rainwater samples and thus

23   may represent nitrate formed aloft. However, since cloud water peaks on average near 1 km altitude in the MERRA2

24   meteorology used to drive GEOS-Chem, our model sampling strategy should capture the majority of the influence of

25   clouds on the chemistry of nitrate formation. The dominant oxidant of NO to NO_2 is O_3 (84-85%). Much of the

26   remaining oxidation occurs due to the reaction with peroxy radicals (HO_2 and RO_2). Oxidation of NO to NO_2 by XO

27   is minor (1%) and occurs over the oceans because the main source of tropospheric reactive halogens is from sea salt

aerosol and sea water (Chen et al., 2017;Sherwen et al., 2016;Wang et al., 2018) (Figure 2). In the model, the global, annual mean lifetime of NO_x in the troposphere against oxidation to nitrate is about 1 day; about 50% of this loss is from the reaction of $NO_2 + OH$. NO_x loss from N_2O_5 becomes more important near the surface where aerosol surface area is relatively high. The global, annual mean lifetime of nitrate in the troposphere against wet and dry deposition to the surface is about 3 days.

For both the "cloud chemistry" and "standard" simulations, the two most important nitrate formation pathways are $NO_2 + OH$ (41-42%) and N_2O_5 hydrolysis (28-41%) , the latter of which is dominant over the mid- to high-northern continental latitudes during winter where both NO_x emissions and aerosol abundances are relatively large (Figures 1 and 3). The "cloud chemistry" simulation results in an equal importance of nitrate formation via $NO_2 + OH$ and N_2O_5 hydrolysis (both 41%) due to increases in the rate of N_2O_5 uptake in clouds and decreases in the importance of NO_2 hydrolysis, which can compete with N_2O_5 formation at night. In the "standard" model, NO_2 hydrolysis represents an important nitrate production mechanism (12%), but it is negligible in the "cloud chemistry" simulation due to the reduction in the reaction probability (from $\gamma_{NO2} = 10^{-4}$ to $\gamma_{NO2} = 10^{-4}$ to 10^{-8}) in the model, which is supported by laboratory studies (Burkholder et al., 2015;Crowley et al., 2010;Tan et al., 2016). The formation of HNO_3 from the hydrolysis of $RONO_2$ formed from both daytime ($NO + RO_2$) and nighttime ($NO_3 + MTN/ISOP$) reactions represents 6% of total, global nitrate formation (Figure 1) and is dominant over Amazonia (Figure 3). $RONO_2$ hydrolysis represents up to 20% of inorganic nitrate formation in the southeast U.S. (Figure 3). This is similar to Fisher et al. (2016) who estimated that formation of $RONO_2$ accounts for up to 20% of NO_x loss in this region during summer, with $RONO_2$ hydrolysis representing 60% of $RONO_2$ loss. Globally, the formation of inorganic nitrate from the hydrolysis of $RONO_2$ is dominated by $RONO_2$ formation from the daytime reactions (3-6%), while the formation of $RONO_2$ from nighttime reactions represents up to 3%. The relative importance of nighttime and daytime $RONO_2$ formation is expressed as a range because precursors to $RONO_2$ that formed from monoterpenes can form from both daytime and nighttime reactions, and these precursors are not separately diagnosed in the model output. HNO_3 formation from $NO_3 + HC$ and the hydrolysis of XNO_3 are small globally (5-6%). Although XNO_3 hydrolysis is the dominant nitrate formation pathway over the remote oceans (Figure 3), its contribution to total, global nitrate production is relatively small due to small local NO_x sources in these regions.

2 Figures 4 - 6 show modeled $\Delta^{17}O$(nitrate) for the "cloud chemistry" simulation (the "standard" simulation is shown in

3 Figures S2 – S4). Figure 4 shows modeled annual-mean $\Delta^{17}O$(nitrate) below 1 km altitude ($\Delta^{17}O(NO_2)$ is shown in

4 Figure S5). The model predicts an annual-mean range of $\Delta^{17}O$(nitrate) = 4 – 33‰ near the surface. The lowest values

5 are over Amazonia due to the dominance of $RONO_2$ hydrolysis and the highest values are over the mid-latitude oceans

6 due to the dominance of XNO_3 hydrolysis (Figures 3 and 4).

8 Figure 5 compares the model with a global compilation of $\Delta^{17}O$(nitrate) observations from around the world.

9 Observations included in Figure 5 include locations where there is enough data to calculate monthly means (McCabe

10 et al., 2006;Kunasek et al., 2008;Hastings et al., 2003;Kaiser et al., 2007;Michalski et al., 2003;Guha et al.,

11 2017;Savarino et al., 2013;Ishino et al., 2017b;Savarino et al., 2007;Alexander et al., 2009;He et al., 2018b;Fibiger et

12 al., 2013;Wang et al., 2014). Figure 6 compares the seasonality in modeled $\Delta^{17}O$(nitrate) to the observations where

13 samples were collected over the course of approximately one year (McCabe et al., 2006;Kunasek et al., 2008;Kaiser

14 et al., 2007;Michalski et al., 2003;Guha et al., 2017;Savarino et al., 2013;Ishino et al., 2017b;Savarino et al.,

15 2007;Alexander et al., 2009). In contrast to Alexander et al. (2009), the model does not significantly underestimate

16 the $\Delta^{17}O$(nitrate) observations when assuming a bulk ozone isotopic composition ($\Delta^{17}O(O_3)$) on the order of 25‰ (see

17 Figure 2d in Alexander et al. (2009)). The increase in modeled $\Delta^{17}O$(nitrate) is due to increased importance of O_3 in

18 NO_x cycling (85% below 1 km) compared to Alexander et al. (2009) (80% below 1 km altitude), and an increase in

19 the number and fractional importance of nitrate formation pathways that yield relatively high values of $\Delta^{17}O$(nitrate)

20 (red pathways in Fig. 1). Although XO species themselves are only a minor NO oxidation pathway (1%), the addition

21 of reactive halogen chemistry in the model has altered the relative abundance of O_3 and HO_x (Sherwen et al., 2016) in

22 such a way as to increase the modeled $\Delta^{17}O(NO_x)$. The Alexander et al. (2009) study used GEOS-Chem v8-01-01,

23 which included tropospheric nitrate formation from the NO + OH, $N_2O_5 + H_2O$, and NO_3 + HC pathways only. An

24 increased importance of N_2O_5 hydrolysis (R4) and additional nitrate formation pathways that yield relatively high

25 values of $\Delta^{17}O$(nitrate) (R5, R6, R8, and R10) in the present study also explain the increase in modeled $\Delta^{17}O$(nitrate)

26 relative to Alexander et al. (2009). An increase in the average A value from 0.80 to 0.85 would tend to increase the

1   calculated $\Delta^{17}O$(nitrate) on the order of 2‰ ($0.05 \times \Delta^{17}O(O_3^*)$), suggesting that the increase in the relative importance

2   of the terminal reactions R4, R5, R6, R8, and R10 explains the majority of the difference between the results presented

3   here compared to (Alexander et al., 2009). Assuming a value of 35‰ for bulk $\Delta^{17}O(O_3)$ in the model that did not

4   include reactive halogen chemistry or heterogeneous reactions in cloud water produced good agreement between

5   modeled and observed $\Delta^{17}O$(nitrate) in Alexander et al. (2009); however, in the current version of the model this bulk

6   isotopic assumption leads to a model overestimate at nearly all locations (Figure S6). The "cloud chemistry" model

7   shows somewhat better agreement with the observations ($R^2 = 0.51$ in Figure 5) compared to the "standard" model

8   ($R^2 = 0.48$ in Figure S3). Improved agreement with the observations occurs in the mid- to high-latitudes (Figures 6

9   and S4) is due to addition of N_2O_5 hydrolysis in clouds (Figures 3 and S6).

11   The mean $\Delta^{17}O$(nitrate) value of the observations (27.7 ± 5.0‰) shown in Figure 5 is not significantly different from

12   the modeled values at the location of the observations (28.6 ± 4.5‰); however, the range of $\Delta^{17}O$(nitrate) values of

13   the observations (10.9 – 40.6‰) is larger than in the model (19.6 – 37.6‰). As previously noted in Savarino et al.

14   (2007), the maximum observed $\Delta^{17}O$(nitrate) value (40.6‰) is not possible given our isotope assumption for the

15   terminal oxygen atom of ozone ($\Delta^{17}O(O_3^*) = 39$‰); however, it is theoretically possible given the approximately 2‰

16   uncertainty in observed $\Delta^{17}O(O_3^*)$. A value of $\Delta^{17}O$(nitrate) = 41‰ is possible if $\Delta^{17}O(O_3^*) = 41$‰ and all oxygen

17   atoms of nitrate originate from ozone ($A = 1$ and all nitrate forms from R2 and/or R5). Although this may be possible

18   for nitrate formed locally in the Antarctic winter due to little to no sunlight, lack of local NO_x sources during Antarctic

19   winter makes it unlikely that all nitrate observed in Antarctica forms locally. Long-range transport from lower latitudes

20   and/or the stratosphere likely contributes to nitrate observed in Antarctica during winter (Lee et al., 2014). Observed

21      $\Delta^{17}O$(nitrate) > 39‰ (in Antarctica) has been suggested to be due to transport of nitrate from the stratosphere (Savarino

22   et al., 2007), as stratospheric O_3 is expected to have a higher $\Delta^{17}O(O_3)$ value than ozone produced in the troposphere

23   (Krankowsky et al., 2000;Mauersberger et al., 2001;Lyons, 2001). Indeed, the model underestimates the observations

24   at Dumont d'Urville (DDU) and the South Pole (both in Antarctica) during winter and spring (Figure 6), when and

25   where the stratospheric contribution is expected to be most important (Savarino et al., 2007). The model underestimate

26   in Antarctica may also be due to model underestimates of BrO column (Chen et al., 2017) and ozone abundance

27   (Sherwen et al., 2016) in the southern high latitudes. The largest model overestimates occur at Mt. Lulin, Taiwan

1 (Figures 5 and 6). Based on nitrogen isotope observations (δ^{15}N), nitrate at Mt. Lulin is thought to be influenced by

2 anthropogenic nitrate emitted in polluted areas of mainland China and transported to Mt. Lulin, rather than local nitrate

3 production (Guha et al., 2017). However, observations of Δ^{17}O(nitrate) in autumn and winter in Beijing suggest much

4 higher values (30.6±1.8‰) than was measured at Mt. Lulin (15 – 30‰ in winter). A potential reason for the model

5 overestimate of the observed values at Mt. Lulin could be qualitatively explained by transport of nitrate formed in the

6 free troposphere to this high altitude location, where the high Δ^{17}O(nitrate) producing pathways (R4-R8) should be

7 negligible due to minimal aerosol surface area for heterogeneous chemistry. Low Δ^{17}O(nitrate) values from nitrate

8 formed at higher altitudes and transported to Mt. Lulin would not be accounted for in the model since the isotopes are

9 not transported. The model compares better to the mid-latitude locations close to pollution sources (La Jolla and

10 Princeton), although the model overestimates wintertime Δ^{17}O(nitrate) in Princeton, NJ, USA by up to 6‰ and

11 underestimates winter time Δ^{17}O(nitrate) in La Jolla, CA, USA by up to 4‰. The model overestimate at Princeton

12 during winter could be due to the fact that these are precipitation samples and not ambient aerosol samples, and thus

13 may reflect nitrate formed at altitudes higher than we are sampling in the model. The underestimate at La Jolla, CA

14 could be due to underestimates in reactive chlorine chemistry in the model, which would tend to increase Δ^{17}O(nitrate)

15 by increasing nitrate formation by the hydrolysis of halogen nitrates (R6) in this coastal location. The model

16 underestimates the Δ^{17}O(nitrate) observations at Cape Verde in late summer/early autumn by up to 6‰ (Savarino et

17 al., 2013). Comparison with results from the steady-state model employed in Savarino et al. (2013) suggests that the

18 low bias could be due to an underestimate of nitrate formation via NO_3 + DMS (R2). The steady-state model in

19 Savarino et al. (2013) agreed with observations when R2 represented about one-third of total nitrate formation. The

20 model results presented here have R2 representing about 15% of total nitrate formation in this season. An

21 underestimate of the relative importance of R2 could result from a model underestimate of atmospheric DMS

22 abundances.

24   **4. Model uncertainties**

25 The uncertainty in the two most important nitrate formation pathways, NO_2 + OH and N_2O_5 hydrolysis, and their

26 impacts on NO_x and oxidant budgets, have been examined and discussed elsewhere (Macintyre and Evans,

27 2010;Newsome and Evans, 2017;Holmes et al., 2019). The impacts of the formation and hydrolysis of halogen nitrates

1   on global NO_x and oxidant budgets have also been previously examined (Sherwen et al., 2016). Here we focus on

2   three additional processes using a set of model sensitivity studies. First, we examine the importance of the third most

3   important nitrate production pathway on the global scale as predicted by the "standard" model, NO_2 aerosol uptake

4   and hydrolysis, and its implications for the global NO_x, nitrate, and oxidant budgets. Second, we examine the role of

5   changing anthropogenic NO_x emissions over a 15-year period (2000 to 2015) on the relative importance of the

6   formation of inorganic nitrate from the hydrolysis of organic nitrates. Finally, we examine the role of aerosol nitrate

7   photolysis on the relative importance of different nitrate formation pathways. The impact of aerosol nitrate photolysis

8   on NO_x and oxidant budgets has been examined in detail elsewhere (Kasibhatla et al., 2018).

10   **4.1 Heterogeneous uptake and hydrolysis of NO_2**

11   Heterogeneous uptake of NO_2 to form HNO_3 and HONO is the third most important nitrate formation pathway in the

12   "standard" model on the global scale (Figure 1). The reaction probability (γ_{NO2}) measured in laboratory studies ranges

13   between 10^{-8} to 10^{-4} depending on aerosol chemical composition (Lee and Tang, 1988;Crowley et al., 2010;Gutzwiller

14   et al., 2002;Yabushita et al., 2009;Abbatt and Waschewsky, 1998;Burkhart et al., 2015;Broske et al., 2003;Li et al.,

15   2018a;Xu et al., 2018). A value of $\gamma_{NO2} = 10^{-4}$ is used in the "standard" model, which is at the high end of the reported

16   range. A molar yield of 0.5 for both HNO_3 and HONO formation is assumed in the model based on laboratory studies

17   and hypothesized reaction mechanisms (Finlayson-Pitts et al., 2003;Jenkin et al., 1988;Ramazan et al., 2004;Yabushita

18   et al., 2009). However, both the reaction rate and mechanism of this reaction and its dependence on chemical

19   composition and pH is still not well understood (Spataro and Ianniello, 2014).

21   The "cloud chemistry" simulation uses a reaction probability formulation for aerosol uptake of NO_2 (γ_{NO2}) that

22   depends on aerosol chemical composition, ranging from $\gamma_{NO2} = 10^{-8}$ for dust to $\gamma_{NO2} = 10^{-4}$ for black carbon based on

23   recent laboratory studies (Holmes et al., 2019). The updated NO_2 reaction probability results in a negligible (<1%)

24   importance of this reaction for nitrate formation, compared to 12% contribution in the "standard" model. The "cloud

25   chemistry" simulation significantly increases the fractional importance of N_2O_5 hydrolysis (from 28 to 41%, globally

26   below 1 km altitude) compared to the "standard" simulation, in part due to decreased competition from NO_2 hydrolysis

27   and in part due to increased N_2O_5 hydrolysis in clouds. To evaluate the relative importance of competition from NO_2

28   hydrolysis and the addition of N_2O_5 hydrolysis in clouds, we perform a model sensitivity study that is the same as the

1   "standard" simulation but decreases the reaction probability of NO_2 hydrolysis on aerosol ($\gamma_{NO2} = 10^{-7}$), without adding

2   N_2O_5 hydrolysis in clouds. Similar to the "cloud chemistry" simulation, using $\gamma_{NO2} = 10^{-7}$ renders NO_2 hydrolysis a

3   negligible nitrate formation pathway, and increases the relative importance of N_2O_5 hydrolysis from 28% to 37%.

4   This suggests that reduced competition from NO_2 hydrolysis is the main reason for the increased importance of N_2O_5

5   hydrolysis in the "cloud chemistry" simulation, though the addition of heterogeneous reactions on clouds also plays a

6   role.

8   NO_2 hydrolysis represents a significant source of HONO in the "standard" model simulation; the reduced NO_2 reaction

9   probability from $\gamma_{NO2} = 10^{-4}$ to $\gamma_{NO2} = 10^{-7}$ results in a reduction of HONO below 1 km altitude by up to 100% over

10   the continents, with relatively small (up to 1 ppb) changes in nitrate concentrations (Figure 7). The reduction in the

11   rate of heterogeneous NO_2 uptake leads to reductions in OH where this reaction was most important in the model

12   (over China and Europe) due to reductions in HONO, but leads to increases in OH elsewhere due to increases in ozone

13   (by up to a few ppb) resulting from small increases in the NO_x lifetime due to a reduction in the NO_x sink (Figure 8).

14   Similar changes in HONO are seen when comparing the "standard" and "cloud chemistry" simulation (not shown).

15   Increased importance of N_2O_5 hydrolysis in both the "cloud chemistry" simulation and the simulation without cloud

16   chemistry but with a reduced reaction probability for NO_2 hydrolysis increases modeled annual-mean $\Delta^{17}O$(nitrate)

17   by up to 3‰ in China where this reaction is most important. This improves model agreement with monthly-mean

18   observations of $\Delta^{17}O$(nitrate) in Beijing (He et al., 2018a) (Figures 5 and S3).

20   The product yields of NO_2 hydrolysis are also uncertain. Jenkin et al. (1988) proposed the formation of a water

21   complex, $NO_2 \cdot H_2O$, leading to the production of HONO and HNO_3. Finlayson-Pitts et al. (2003) and Ramazan et al.

22   (2004) proposed the formation of the dimer N_2O_4 on the surface, followed by isomerization to form $NO^+NO_3^-$.

23   Reaction of $NO^+NO_3^-$ with H_2O results in the formation of HONO and HNO_3. Laboratory experiments by Yabushita

24   et al. (2009) suggested that dissolved anions catalyzed the dissolution of NO_2 to form a radical intermediate $X-NO_2^-$

25   (where X = Cl, Br, or I) at the surface followed by reaction with NO_2(g) to form HONO and NO_3^-. These experiments

26   described above were performed at NO_2 concentrations much higher than exist in the atmosphere (10 – 100 ppm)

27   (Yabushita et al., 2009;Finlayson-Pitts et al., 2003;Ramazan et al., 2004). A laboratory study utilizing isotopically

28   labeled water to investigate the reaction mechanism suggested that the formation of HONO resulted from the reaction

between adsorbed NO_2 and H^+, while the formation of HNO_3 resulted from the reaction between adsorbed NO_2 and OH^-, and did not involve the N_2O_4 intermediate (Gustafsson et al., 2009). Results from Gustafsson et al. (2009) suggest an acidity-dependent yield of HONO and HNO_3, favoring HONO at low pH values. A recent study in the northeast U.S. during winter found that modeled nitrate abundance was overestimated using a molar yield of 0.5 for HONO and HNO_3, and the model better matched the observations of NO_2 and nitrate when assuming a molar yield of 1.0 for HONO (Jaeglé et al., 2018). Particles were acidic (pH < 2) during this measurement campaign (Guo et al., 2017;Shah et al., 2018), which may favor HONO production over HNO_3.

We examine the potential importance of this acidity-dependent yield by implementing a pH-dependent product yield in two separate sensitivity simulations, first using an NO_2 aerosol uptake reaction probability of $\gamma = 10^{-4}$ as in the "standard" simulation and second with $\gamma_{NO2} = 10^{-7}$. The acidity-dependent yield for HONO and HNO_3 formation is based on the laboratory study by Gustafsson et al. (2009). We use aerosol pH calculated from ISORROPIA II (Fountoukis and Nenes, 2007) to calculate the concentration of $[H^+]$ and $[OH^-]$ in aerosol water. The yield of HONO (Y_{HONO}) from heterogeneous uptake of NO_2 on aerosol surfaces is calculated according to E3:

$$Y_{HONO} = \frac{[H^+]}{[H^+]+[OH^-]} \tag{E3}$$

where $[H^+]$ and $[OH^-]$ are in units of M. The yield of HNO_3 from this reaction is equal to $(1 - Y_{HONO})$. E3 yields values of Y_{HONO} near unity for aerosol pH values less than 6, decreasing rapidly to zero between pH values between 6-8 (Figure S8). Calculated aerosol pH values are typically < 6 in the model except in remote regions far from NO_x sources (Figure S9), favoring the product HONO.

The acidity-dependent yield implemented in the "standard" simulation with $\gamma_{NO2} = 10^{-4}$ increases HONO concentrations by up to 1 ppbv in China where this reaction is most important (Figure 9). Fractional increases in HONO exceed 100% in remote locations (Figure 9). Increased HONO leads to increases in OH on the order of 10 – 20% in most locations below 1 km altitude, while ozone concentrations increase in most locations by up to several ppbv (Figure 9). The exception is the southern high latitudes; likely due to decreased formation and thus transport of nitrate to remote locations. The impact on NO_x and nitrate budgets is relatively minor. The global, annual mean NO_x burden near the surface (below 1 km) increases slightly (+2%) as a result of the decreased rate of conversion of NO_2 to nitrate; the change to the global tropospheric burden is negligible. Annual-mean surface nitrate concentrations

1 show small decreases up to 1 ppbv in China where this reaction is most important in the model; impacts on nitrate

2 concentrations over a shorter time period may be more significant (Jaeglé et al., 2018). The fraction of HNO_3 formed

3 from NO_2 + OH (49%) increases due to increases in OH from the HONO source. The fraction of HNO_3 formation

4 from the uptake and hydrolysis of N_2O_5 also increases (from 28% to 32%) due to reductions in the nighttime source

5 of nitrate from NO_2 hydrolysis. The calculated mean $\Delta^{17}O$(nitrate) at the location of the observations shown in Figure

6 5 (27.9 ± 5.0‰) is not significantly impacted due to compensating effects from changes in both high- and low-

7 producing $\Delta^{17}O$(nitrate) values. Modeled monthly mean $\Delta^{17}O$(nitrate) in China, where NO_2 hydrolysis is most

8 important decreases by 0.9-1.9‰, and is biased low by 1.8-3.4‰.

10 Using a combination of both the low reaction probability ($\gamma = 10^{-7}$) and the acidity-dependent yield gives similar results

11 as using $\gamma = 10^{-7}$ and assuming a molar yield of 0.5 for HONO and HNO_3 (not shown). In other words, including a

12 pH-dependent product yield rather than a yield of 0.5 for HONO and nitrate results in negligible differences for

13 oxidants, NO_x and nitrate abundances when the reaction probability (γ_{NO2}) is low.

15 **4.2 Hydrolysis of organic nitrates ($RONO_2$)**

16 Anthropogenic NO_x emissions have been increasing in China and decreasing in the U.S. and Europe (Richter et al.,

17 2005;Hoesly et al., 2018b), with implications for the relative importance of inorganic and organic nitrate formation as

18 a sink for NO_x (Zare et al., 2018). To examine the impacts of recent changes in anthropogenic NO_x emissions for

19 nitrate formation pathways, we run the "standard" model using the year 2000 emissions and meteorology after a 1-

20 year model spin up, and compare the results to the "standard" model simulation run in the year 2015. This time-period

21 encompasses significant changes in anthropogenic NO_x emissions in the U.S., Europe, and China, and encompasses

22 most of the time period of the observations shown in Figures 5 and 6. Total, global anthropogenic emissions of NO_x

23 are slightly lower in the 2000-year simulation (30 Tg N yr^{-1}) compared to the year 2015 simulation (31 Tg N yr^{-1}) due

24 to decreases in North America and Europe, counteracted by increases in Asia (Figure S10). This leads to increases of

25 less than 10% in the annual-mean, fractional importance of the source of nitrate from the hydrolysis of organic nitrates

26 in the U.S., and corresponding decreases of less than 10% over China (Figure 10). Relatively small changes (< 10%)

27 in nitrate formation pathways yield small changes (< 2‰) in modeled annual-mean $\Delta^{17}O$(nitrate) between the year

28 2000 and 2015, differences in $\Delta^{17}O$(nitrate) over shorter time periods may be larger. Changes in the formation of

1   nitrate from the hydrolysis of $RONO_2$ remains unchanged globally, as increases in the U.S. and Europe and decreases

2   in China counteract one another.

4   **4.3 Photolysis of aerosol nitrate**

5   Observations have demonstrated that aerosol nitrate can be photolyzed at rates much faster than $HNO_3(g)$ (Reed et al.,

6   2017;Ye et al., 2016); however, the magnitude of the photolytic rate constant is uncertain.   We examine the

7   implications of this process for global nitrate formation pathways by implementing the photolysis of aerosol nitrate as

8   described in Kasibhatla et al. (2018) into the "standard" model simulation, scaling the photolytic rate constant for both

9   fine- and coarse-mode aerosol nitrate to a factor of 25 times higher than that for $HNO_3(g)$ (Kasibhatla et al.,

10   2018;Romer et al., 2018), with a molar yield of 0.67 for HONO and 0.33 for NO_x production.   The global, annual

11   mean NO_x burden near the surface (below 1 km) increases slightly (+2%) as a result of the photolytic recycling of

12   nitrate to NO_x, similar to Kasibhatla et al. (2018).   Aerosol nitrate photolysis results in only small impacts on the

13   relative importance of nitrate formation pathways (< 2%) likely due to simultaneous increases in O_3 and OH

14   (Kasibhatla et al., 2018), which in turn yields small impacts on calculated $\Delta^{17}O$(nitrate) at the location of the

15   observations shown in Figure 5 (27.9 ± 5.0‰).   Nitrate photolysis itself has minimal impact on $\Delta^{17}O$(nitrate) because

16   it is a mass-dependent process (McCabe et al., 2005).

18   **5   Conclusions**

19   Observations of $\Delta^{17}O$(nitrate) can be used to help quantify the relative importance of different nitrate formation

20   pathways.   Interpretation of $\Delta^{17}O$(nitrate) requires knowledge of $\Delta^{17}O(O_3)$.   Previous modeling studies showed good

21   agreement between observed and modeled $\Delta^{17}O$(nitrate) when assuming a bulk oxygen isotopic composition of ozone

22   ($\Delta^{17}O(O_3)$) of 35‰ based on laboratory and modeling studies (Morton et al., 1990;Thiemens, 1990;Lyons, 2001).

23   However, recent and spatially widespread observations of $\Delta^{17}O(O_3)$ have consistently shown $\Delta^{17}O(O_3) = 26 \pm 1‰$,

24   suggesting that models are underestimating the role of ozone relative to HO_x in NO_x chemistry.   We utilize a global

25   compilation of observations of $\Delta^{17}O$(nitrate) to assess the representation of nitrate formation in a global chemical

26   transport model (GEOS-Chem), assuming that the bulk oxygen isotopic composition of ozone ($\Delta^{17}O(O_3)$) = 26‰.

27   The modeled $\Delta^{17}O$(nitrate) is roughly consistent with observations, with a mean modeled and observed $\Delta^{17}O$(nitrate)

28   of (28.6 ± 4.5‰) and (27.6 ± 5.0‰), respectively, at the locations of the observations.   Improved agreement between

modeled and observed $\Delta^{17}O$(nitrate) is due to increased importance of ozone versus HO_2 and RO_2 in NO_x cycling and an increase in the number and importance of nitrate production pathways that yield high $\Delta^{17}O$(nitrate) values. The former may be due to implementation of tropospheric reactive halogen chemistry in the model, which impacts ozone and HO_x abundances. The latter is due mainly to increases in the relative importance of N_2O_5 hydrolysis, with the hydrolysis of halogen nitrates also playing an important role in remote regions.

The main nitrate formation pathways in the model below 1 km altitude are from $NO_2 + OH$ and N_2O_5 hydrolysis (both 41%). The relative importance of global nitrate formation from the hydrolysis of halogen nitrates and hydrogen-abstraction reactions involving the nitrate radical (NO_3) are of similar magnitude (~5%). The formation of nitrate from the hydrolysis of organic nitrate has increased slightly in the U.S. and decreased in China (changes <10%) due to changing NO_x emissions from the year 2000 to 2015, although the global mean fractional importance (6%) remains unchanged as the regional changes counteract one another. Nitrate formation via heterogeneous NO_2 and NO_3 uptake and $NO_2 + HO_2$ are negligible (<2%). Although aerosol nitrate photolysis has important implications for O_3 and OH, the impacts on nitrate formation pathways are small.

The model parameterization for heterogeneous uptake of NO_2 has significant impacts on HONO and oxidants (OH and ozone) in the model. HONO production from this reaction has been suggested to be an important source of OH in Chinese haze due to high NO_x and aerosol abundances (Hendrick et al., 2014;Tong et al., 2016;Wang et al., 2017), with implications for the gas-phase formation of sulfate aerosol from the oxidation of sulfur dioxide by OH (Shao et al., 2019;Li et al., 2018b). More recent laboratory studies suggest that the reaction probability of NO_2 on aerosols is lower than that previously used in the model. Using an NO_2 reaction probability formulation that depends on the chemical composition of aerosols as described in Holmes et al. (2019) renders this reaction negligible for nitrate formation, and has significant implications for modeled HONO, ozone, and OH. Although uncertainty also exists in the relative yield of nitrate and HONO from this reaction, the impacts of this assumption are negligible when we use these updated NO_2 reaction probabilities. Observations of $\Delta^{17}O$(nitrate) in Chinese haze events during winter (He et al., 2018b) may help to quantify the importance of this nitrate production pathway in a region where the model predicts it is significant.

1 Data availability: The GEOS-Chem model is available at http://acmg.seas.harvard.edu/geos.

3 Author contributions: B.A. designed the study and performed the model simulations and calculations. All other

4 authors provided model code and contributed to writing and analysis.

6 Competing interests: The authors declare that they have no conflict of interest.

8 **Acknowledgements**:

9 B.A. acknowledges NSF AGS 1644998 and 1702266 and helpful discussions with Joël Savarino and Ron Cohen.

10 C.D.H. acknowledges the NASA New Investigator Program grant NNX16AI57G. J.A.F. acknowledges Australian

11 Research Council funding DP160101598.

13 **References**

14 Abbatt, J. P. D., and Waschewsky, G. C. G.: Heterogeneous interactions of OHBr, HNO_3, O_3, and NO_2 with
15 deliquescent NaCl aerosols at room temperature, J. Phys. Chem. A, 102, 3719-3725, 1998.
16 Alexander, B., Savarino, J., Kreutz, K. J., and Thiemens, M. H.: Impact of preindustrial biomass-burning
17 emissions on the oxidation pathways of tropospheric sulfur and nitrogen, J. Geophys. Res., 109, D08303,
18 doi: 10.1029/2003JD004218, 2004.
19 Alexander, B., Hastings, M. G., Allman, D. J., Dachs, J., Thornton, J. A., and Kunasek, S. A.: Quantifying
20 atmospheric nitrate formation pathways based on a global model of the oxygen isotopic composition
21 ($\Delta^{17}O$) of atmospheric nitrate, Atmos. Chem. Phys., 9, 5043-5056, 10.5194/acp-9-5043-2009, 2009.
22 Atkinson, R.: Atmospheric chemistry of VOCs and NOx, Atm. Env., 34, 2063-2101, 10.1016/S1352-
23 2310(99)00460-4, 2000.
24 Berhanu, T. A., Savarino, J., Bhattacharya, S. K., and Vicars, W. C.: ^{17}O excess transfer during the $NO_2 + O_3$
25 --> $NO_3 + O_2$ reaction, J. Chem. Phys., 136, 044311, doi: 10.1063/1.3666852, 2012.
26 Bertram, T. H., and Thornton, J. A.: Toward a general parameterization of N2O5 reactivity on aqueous
27 particles: the competing effects of particle liquid water, nitrate and chloride, Atmos. Chem. Phys, 9,
28 8351-8363, 10.5194/acp-9-8351-2009, 2009.
29 Bey, I., Jacob, D. J., Yantosca, R. M., Logan, J. A., Field, B. D., Fiore, A. M., Li, Q., Liu, H. Y., Mickley, L. J.,
30 and Schultz, M. G.: Global modeling of tropospheric chemistry with assimilated meteorology: Model
31 description and evaluation, J. Geophys. Res., 106, 23073-23095, 2001.
32 Bhattacharya, S. K., Pandey, A., and Savarino, J.: Determination of intramolecular isotope distribution of
33 ozone by oxidation reaction with silver metal, J. Geophys. Res, 113, D03303, doi:10.1029/2006JF008309,
34 2008.
35 Bhattacharya, S. K., Savarino, J., Michalski, G., and Liang, M.-C.: A new feature in the internal heavy
36 isotope distribution in ozone, J. Chem. Phys., 141, 10.1063/1.4895614, 2014.
37 Brenninkmeijer, C. A. M., Janssen, C., Kaiser, J., Rockmann, T., Rhee, T. S., and Assonov, S. S.: Isotope
38 effects in the chemistry of atmospheric trace compounds, Chemical Reviews, 102, 5125-5161, 2003.

1   Broske, R., Kleffmann, J., and Wiesen, P.: Heterogeneous conversion of NO2 on secondary organic
2   aerosol surfaces: A possible source of nitrous acid (HONO) in the atmosphere?, Atmos. Chem. Phys, 3,
3   469-474, 10.5194/acp-3-469-2003, 2003.
4   Brothers, L. A., Dominguez, G., Fabian, P., and Thiemens, M. H.: Using multi-isotope tracer methods to
5   understand the sources of nitrate in aerosols, fog and river water in Podocarpus National Forest,
6   Ecuador, Eos Trans. AGU, 89, Abstract A11C-0136, 2008.
7   Browne, E. C., and Cohen, R. C.: Effects of biogenic nitrate chemistry on the NOx lifetime in remost
8   continental regions, Atmos. Chem. Phys, 12, 11917-11932, 10.5194/acp-12-11917-2012, 2014.
9   Burkhart, J. F., Sander, S. P., Abbatt, J. P. D., Barker, J. R., Huie, R. E., Kolb, C. E., Kurylo, M. J., Orkin, V. L.,
10   Wilmouth, D. M., and Wine, P. H.: Chemical Kinetics and Photochemical Data for Use in Atmospheric
11   Studies, Jet Propulsion Laboratory, Pasadena, CA, USA, 2015.
12   Burkholder, J. B., Sander, S. P., Abbatt, J. P. D., Barker, J. R., Huie, R. E., Kolb, C. E., Kurylo, M. J., Orkin, V.
13   L., Wilmouth, D. M., and Wine, P. H.: Chemical kinetics and photochemical data for use in atmospheric
14   studies: evaluation number 18, Jet Propulsion Laboratory, Pasadena, CA, 2015.
15   Butkovskaya, N. I., Kukui, A., Pouvesle, N., and Le Bras, G.: Formation of Nitric Acid in the Gas-Phase HO_2
16   + NO Reaction: Effects of Temperature and Water Vapor, J. Phys. Chem. A, 109, 6509-6520,
17   10.1021/jp051534v, 2005.
18   Chen, Q., Schmidt, J. A., Shah, V., Jaeglé, L., Sherwen, T., and Alexander, B.: Sulfate production by
19   reactive bromine: Implications for the global sulfur and reactive bromine budgets, Geophys. Res. Lett.,
20   44, 7069-7078, 10.1002/2017GL073812, 2017.
21   Chen, Q., Edebeli, J., McNamara, S. M., Kulju, K., May, N. W., Bertman, S. P., Thanekar, S., Fuentes, J. D.,
22   and Pratt, K. A.: HONO, Particulate Nitrite, and Snow Nitrite at a Midlatitude Urban Site during
23   Wintertime, ACS Earth Space Chem., 10.1021/acsearthspacechem.9b00023, 2019.
24   Connell, P., and Johnston, H. S.: Thermal dissociation of N_2O_5 in N_2, Geophys. Res. Lett., 6, 553-556,
25   1979.
26   Costa, A. W., Michalski, G., Schauer, A. J., Alexander, B., Steig, E. J., and Shepson, P. B.: Analysis of
27   atmospheric inputs of nitrate to a temperate forest ecosystem from $\Delta^{17}O$ isotope ratio measurements,
28   Geophys. Res. Lett., 38, L15805, doi:10.1029/2011GL047539, 2011.
29   Crowley, J. N., Ammann, M., Cox, R. A., Hynes, R. G., Jenkin, M. E., Mellouki, A., Rossi, M. J., Troe, J., and
30   Wallington, T. J.: Evaluated kinetic and photochemical data for atmospheric chemistry: Volume V –
31   heterogeneous reactions on solid substrates, Atmos. Chem. Phys, 10, 9059-9223, 10.5194/acp-10-9059-
32   2010, 2010.
33   Domine, F., and Shepson, P. B.: Air-Snow Interactions and Atmospheric Chemistry, Science, 297, 1506,
34   2002.
35   Dubey, M. K., Mohrschladt, R., Donahue, N. M., and Anderson, J. G.: Isotope-specific kinetics of hydroxyl
36   radical (OH) with water (H_2O): Testing models of reactivity and atmospheric fractionation, J. Phys. Chem.
37   A, 101, 1494-1500, 1997.
38   Evans, M. J., and Jacob, D. J.: Impact of new laboratory studies of N_2O_5 hydrolysis on global model
39   budgets of tropospheric nitrogen oxides, ozone, and OH, Geophys. Res. Lett., 32, L09813,
40   doi:10.1029/2005GL022469, 2005.
41   Ewing, S. A., Michalski, G., Thiemens, M., Quinn, R. C., Macalady, J. L., Kohl, S., Wankel, S. D., Kendall, C.,
42   McKay, C. P., and Amundson, R.: Rainfall limit of the N cycle on Earth, Global Biogeochemical Cycles, 21,
43   GB3009, 10.1029/2006gb002838, 2007.
44   Fibiger, D. L., Hastings, M. G., Dibb, J. E., and Huey, L. G.: The preservations of atmospheric nitrate in
45   snow at Summit, Greenland, Geophys. Res. Lett., 40, 3484-3489, 10.1002/grl.50659, 2013.
46   Finlayson-Pitts, B. J., Wingen, L. M., Sumner, A. L., Syomin, D., and Ramazan, K. A.: The heterogeneous
47   hydrolysis of NO_2 in laboratory systems and in outdoor and indoor atmospheres: An integrated
48   mechanism, Phys. Chem. Chem. Phys., 5, 223-242, 2003.

Fisher, J. A., Jacob, D. J., Travis, K. R., Kim, P. S., Marais, E. A., Miller, C. C., Yu, K., Zhu, L., Yantosca, R. M., Sulprizio, M. P., Mao, J., Wennberg, P. O., Crounse, J. D., Teng, A. P., Nguyen, T. B., St. Clair, J. M., Cohen, R. C., Romer, P., Nault, B. A., Wooldridge, P. J., Jimenez, J. L., Campuzano-Jost, P., D.A., D., Hu, W., Shepson, P. B., Wiong, F., Blake, D. R., Goldstein, A. H., Misztal, P. K., Hanisco, T. F., Wolfe, G. M., Ryerson, T. B., Wisthaler, A., and Mikoviny, T.: Organic nitrate chemistry and its implications for niteogen budgets in an isoprene- and mooterpene-rich atmosphere: constraints from aircraft (SEAC^{4}RS) and ground-based (SOAS) observations in the Southeast US, Atmos. Chem. Phys, 16, 5969-5991, 10.5194/acp-16-5969-2016, 2016.

Fisher, J. A., Atlas, E. L., Barletta, B., Meinardi, S., Blake, D. R., Thompson, C. R., Ryerson, T. B., Peischl, J., Tzompa-Sosa, Z. A., and Murray, L. T.: Methyl, Ethyl, and Propyl Nitrates: Global Distribution and Impacts on Reactive Nitrogen in Remote Marine Environments, J. Geophys. Res., 123, 12,429-412,451, doi.org/10.1029/2018JD029046, 2018.

Fountoukis, C., and Nenes, A.: ISORROPIA II: a computationally efficient thermodynamic equilibrium model for K^+-Ca^{2+}-Mg^{2+}-NH_4^+-Na^+-SO_4^{2-}-NO_3^--Cl^--H_2O aerosols, Atmos. Chem. Phys., 7, 4639-4659, 2007.

Geng, L., Cole-Dai, J., Alexander, B., Savarino, J., Schauer, A. J., Steig, E. J., Lin, P., and Zatko, M. C.: On the origin of the occasional springtime nitrate concentration maximum in Greenland snow, Atmos. Chem. Phys. Discuss., 14, 9401-9437, 10.5194/acpd-14-9401-2014, 2014.

Geng, L., Murray, L. T., Mickley, L. J., Lin, P., Fu, Q., Schauer, A. J., and Alexander, B.: Isotopic evidence of multiple controls on atmospheric oxidants over climate transitions, Nature, 546, 133-136, 10.1038/nature22340, 2017.

Guha, T., Lin, C. T., Bhattacharya, S. K., Mahajan, A. S., Ou-Yang, C.-F., Lan, Y.-P., Hsu, S. C., and Liang, M.-C.: Isotopic ratios of nitrate in aerosol samples from Mt. Lulin, a high-altitude station in Central Taiwan, Atmos. Env., 154, 53-69, 10.1016/j.atmosenv.2017.01.036, 2017.

Guo, H., Weber, R. J., and Nenes, A.: High levels of ammonia do not raise fine particle pH sufficiently to yield nitrogen oxide-dominated sulfate production, Scientific Reports, 7, 1-7, 10.1038/s41598-017-11704-0, 2017.

Gustafsson, R. J., Kyiakou, G., and Lambert, R. M.: The molecular methanism of tropospheric nitrous acid production on mineral dust surfaces, Chem. Phys. Chem., 9, 1390-1393, 10.1002/cphc.200800259, 2009.

Gutzwiller, L., George, C., Rossler, E., and Ammann, J.: Reaction Kinetics of NO_2 with Resorcinol and 2,7-Naphthalenediol in the Aqueous Phase at Different pH, J. Phys. Chem. A, 106, 12045-12050, 10.1021/jp026240d, 2002.

Hastings, M. G., Sigman, D. M., and Lipschultz, F.: Isotopic evidence for source changes of nitrate in rain at Bermuda, J. Geophys. Res., 108, 4790, doi:10.1029/2003JD003789, 2003.

He, P., Alexander, B., Geng, L., Chi, X., Fan, S., Zhan, H., Kang, H., Zheng, G., Cheng, Y., Su, H., Liu, C., and Xie, Z.: Isotopic constraints on heterogeneous sulfate production in Beijing haze, Atmos. Chem. Phys, 18, 5515-5528, 10.5194/acp-18-5515-2018 2018a.

He, P., Xie, Z., Chi, X., Yu, X., Fan, S., Kang, H., Liu, C., and Zhan, H.: Atmospheric $\Delta^{17}O(NO_3^-)$ reveals nocturnal chemistry dominates nitrate production in Beijing haze, Atmos. Chem. Phys, 18, 14465–14476, 10.5194/acp-18-14465-2018, 2018b.

Heidenreich, J. E., and Thiemens, M. H.: A non-mass dependent oxygen isotope effect in the production of ozone from molecular oxygen: The role of molecular symmetry in isotope chemistry, J. Chem. Phys., 84, 2129-2136, 1986.

Hendrick, F., Muller, J.-F., Clemer, K., Wang, P., De Maziere, M., Fayt, C., Gielen, C., Hermans, C., Ma, J. Z., Pinardi, G., Stavrakou, T., Vlemmix, T., and Van Roosendael, M.: Four years of ground-based MAX-DOAS observations of HONO and NO_2 in the Beijing area, Atmos. Chem. Phys, 14, 765-781, 10.5194/acp-14-765-2014, 2014.

Hoesly, R. M., Smith, S. J., Feng, L., Klimont, Z., Janssens-Maenhout, G., Pitkanen, T., Seibert, J. J., Vu, L., Andres, R. J., Bolt, R. M., Bond, T. C., Dawidowski, L., Kholod, N., Kurokawa, J.-I., Li, M., Liu, L., Lu, Z.,

Moura, M. C. P., O'Rourke, P. R., and Zhang, Q.: Historical (17502014) anthropogenic emissions of reactive gases and aerosols from the Community Emissions Data System (CEDS), Geosci. Model Dev., 11, 369-408, 10.5194/gmd-11-369-2018, 2018a.

Hoesly, R. M., Smith, S. J., Feng, L., Klimont, Z., Janssens-Maenhout, G., Pitkanen, T., Seibert, J. J., Vu, L., Andres, R. J., Bolt, R. M., Bond, T. C., Dawidowski, L., Kholod, N., Kurokawa, J., Li, M., Liu, L., Lu, Z., Moura, M. C. P., O'Rourke, P. R., and Zhang, Q.: Historical (1750–2014) anthropogenic emissions of reactive gases and aerosols from the Community Emissions Data System (CEDS), Geosci. Model Dev., 11, 369-408, 10.5194/gmd-11-369-2018, 2018b.

Holmes, C. D., Prather, M. J., and Vinken, G. C. M.: The climate impact of ship NOx emissions: an improved estimate accounting for plume chemistry, Atmos. Chem. Phys, 14, 6801-6812, 10.5194/acp-14-6801-2014, 2014.

Holmes, C. D., Bertram, T. H., Confer, K. L., Graham, K. A., Ronan, A. C., Wirks, C. K., and Shah, V.: The role of clouds in the tropospheric NOx cycle: a new modeling approach for cloud chemistry and its global implications, Geophys. Res. Lett., 46, GL081990, 10.1029/2019GL081990, 2019.

Horowitz, L. W., Fiore, A. M., Milly, G. P., Cohen, R. C., Perring, A., Wooldridge, P. J., Hess, P. G., Emmons, L. K., and Lamarque, J.-F.: Observational constraints on the chemistry of isoprene nitrates over the eastern United States, J. Geophys. Res, 112, D12S08, doi:10.1029/2006JD007747, 2007.

Hudman, R. C., Moore, N. E., Martin, R. V., Russell, A. R., Mebust, A. K., Valin, L. C., and Cohen, R. C.: A mechanistic model of global soil nitric oxide emissions: implementation and space based-constraints, Atmos. Chem. Phys, 12, 7779-7795, 10.5194/acp-12-7779-2012, 2012.

Ishino, S., Hattori, S., Savarino, J., Jourdain, B., Preunkert, S., Legrand, M., Caillon, N., Barbero, A., Kuribayashi, K., and Yoshida, N.: Seasonal variations of triple oxygen isotopic compositions of atmospheric sulfate, nitrate, and ozone at Dumont d'Urville, coastal Antarctica, Atmos. Chem. Phys, 17, 3713-3727, 10.5194/acp-17-3713-2017, 2017a.

Ishino, S., Hattori, S., Savarino, J., Jourdain, B., Preunkert, S., Legrand, M., Caillon, N., Barbero, A., Kurlbayashi, K., and Yoshida, N.: Seasonal variations of triple oxygen isotopic compositions of atmospheric sulfate, nitrate, and ozone at Dumont d'Urville, coastal Antarctica, Atmos. Chem. Phys, 17, 3713-3727, 10.5194/acp-17-3713-2017, 2017b.

Jacob, D. J.: Heterogeneous chemistry and tropospheric ozone, Atmos. Env., 34, 2131-2159, 2000.

Jacobs, M. I., Burke, W. J., and Elrod, M. J.: Kinetics of the reactions of isoprene-derived hydroxynitrates: gas phase epoxide formation and solution phase hydrolysis,, Atmos. Chem. Phys, 2014, 8933–8946, 10.5194/acp-14-8933-2014, 2014.

Jaeglé, L., Steinberger, L., Martin, R. V., and Chance, K.: Global partitioning of NO_x sources using satellite observations: Relative roles of fossil fuel combustion, biomass burning and soil emissions, Faraday Discussions, 130, 407-423, DOI: 10.1039/b502128f, 2005.

Jaeglé, L., Shah, V., Thornton, J. A., Lopez-Hilfiker, F. D., Lee, B. H., McDuffie, E. E., Fibiger, D., Brown, S. S., Veres, P., Sparks, T. L., Ebben, C. J., Wooldridge, P. J., Kenagy, H. S., Cohen, R. C., Weinheimer, A. J., Campos, T. L., Montzka, D. D., Digangi, J. P., Wolfe, G. M., Hanisco, T., Schroder, J. C., Campuzano-Jost, P., Day, D. A., Jimenez, J. L., Sullivan, A. P., Guo, H., and Weber, R. J.: Nitrogen oxides emissions, chemistry, deposition, and export over the Northeast United States during the WINTER aircraft campaign, J. Geophys. Res., 123, 12,368–312,393, doi.org/10.1029/2018JD029133, 2018.

Jenkin, M. E., Cox, R. A., and Williams, D. J.: Laboratory studies of the kinetics of formation of nitrous acid from the thermal reaction of nitrogen dioxide and water vapor, Atm. Env., 22, 487-498, 1988.

Johnston, J. C., and Thiemens, M. H.: The isotopic composition of tropospheric ozone in three environments, J. Geophys. Res., 102, 25395-25404, 1997.

Kaiser, J., Hastings, M. G., Houlton, B. Z., Rockmann, T., and Sigman, D. M.: Triple Oxygen Isotope Analysis of Nitrate Using the Denitrifier Method and Thermal Decomposition of N_2O, Anal. Chem., 79, 599-607, 2007.

Kasibhatla, P., Sherwen, T., Evans, M. J., Carpenter, L. J., Reed, C., Alexander, B., Chen, Q., Sulprizio, M. P., Lee, J. D., Read, K. A., Bloss, W. J., Crilley, L. R., Keene, W. C., Pzenny, A. A. P., and Hodzic, H.: Global impact of nitrate photolysis of sea-salt aerosol on NOx, OH and ozone in the marine boundary layer, Atmos. Chem. Phys, 18, 11185-11203, 10.5194/acp-18-11185-2018 2018.

Krankowsky, D., Bartecki, F., Klees, G. G., Mauersberger, K., Schellenback, K., and Stehr, J.: Measurement of heavy isotope enrichment in tropospheric ozone, Geophys. Res. Lett., 22, 1713-1716, 1995.

Krankowsky, D., Lammerzahl, P., and Mauersberger, K.: Isotopic measurements of stratospheric ozone, Geophys. Res. Lett., 27, 2593-2595, 2000.

Kunasek, S. A., Alexander, B., Hastings, M. G., Steig, E. J., Gleason, D. J., and Jarvis, J. C.: Measurements and modeling of $\Delta^{17}O$ of nitrate in a snowpit from Summit, Greenland, J. Geophys. Res. , 113, D24302, 10.1029/2008JD010103, 2008.

Lee, C., Martin, R. V., van Donkelaar, A., Lee, H., Dickerson, R. R., Hains, J. C., Krotkov, N., Richter, A., innikov, K., and Schwab, J. J.: SO_2 emissions and lifetimes: Estimates from inverse modeling using in situ and global, space-based (SCIAMACHY and OMI) observations, J. Geophys. Res., 116, D06304, 10.1029/2010JD014758, 2011.

Lee, H.-M., Henze, D. K., Alexander, B., and Murray, L. T.: Investigating the sensitivity of surface-level nitrate seasonality in Antarctica to primary sources using a global model, Atm. Env., 89, 757-767, 10.1016/j.atmosenv.2014.03.003, 2014.

Lee, J. H., and Tang, I. N.: Accommodation coefficient of gaseous NO_2 on water surfaces, Atm. Env., 22, 1988.

Levy, H., Moxim, W. J., Klonecki, A. A., and Kasibhatla, P. S.: Simulated tropospheric NOx: Its evaluation, global distribution and individual source contributions, J. Geophys. Res, 104, 26,279-226,306, 1999.

Li, L., Duan, Z., Li, H., Zhu, C., Henkelman, G., Francisco, J. S., and Zeng, X. C.: Formation of HONO from the NH3-promoted hydrolysis

of NO2 dimers in the atmosphere, Proc. Natl. Acad. Sci., 115, 7236–7241, 10.1073/pnas.1807719115, 2018a.

Li, L., Hoffmann, M. R., and Colussi, A. J.: Role of Nitrogen Dioxide in the Production of Sulfate during Chinese Haze-Aerosol Episodes, Env. Sci. & Tech., 52, 2686-2693, 10.1021/acs.est.7b05222, 2018b.

Li, M., Q. Zhang, J. Kurokawa, J. H. Woo, K. B. He, Z. Lu, T. Ohara, Y. Song, D. G. Streets, G. R. Carmichael, Y. F. Cheng, C. P. Hong, H. Huo, X. J. Jiang, S. C. Kang, F. Liu, H. Su, and Zheng, B.: MIX: a mosaic Asian anthropogenic emission inventory for the MICS-Asia and the HTAP projects, Atmos. Chem. Phys, 17, 935-963, 10.5194/acp-17-935-2017, 2017.

Liang, J., Horowitz, L. W., Jacob, D. J., Wang, Y., Fiore, A. M., Logan, J. A., Gardner, G. M., and Munger, J. W.: Seasonal budgets of reactive nitrogen species and ozone over the United States, and export fluxes to the global atmosphere,, J. Geophys. Res., 103, 13435–13450,, 1998.

Liu, H., Jacob, D. J., Bey, I., and Yantosca, R. M.: Constraints from ^{210}Pb and [7]Be on wet deposition and transport in a global three-dimensional chemical tracer model driven by assimilated meteorological fields, J. Geophys. Res., 106, 12,109-112,128, 2001.

Long, M. S., Keene, W. C., Easter, R. C., Sander, R., Liu, X., Kerkweg, A., and Erickson, D.: Sensitivity of tropospheric chemical composition to halogen-radical chemistry using a fully coupled size-resolved multiphase chemistry-global climate system: halogen distributions, aerosol composition, and sensitivity of climate-relevant gases, Atmos. Chem. Phys, 14, 3397-3425, 10.5194/acp-14-3397-2014, 2014.

Lyons, J. R.: Transfer of mass-independent fractioation on ozone to other oxygen-containing molecules in the atmosphere, Geophys. Res. Lett., 28, 3231-3234, 2001.

Macintyre, H. L., and Evans, M. J.: Sensitivity of a global model to the uptake of N2O5 by tropospheric aerosol, Atmos. Chem. Phys, 10, 7409-7401, 10.5194/acp-10-7409-2010, 2010.

1   Martin, R. V., Jacob, D. J., Yantosca, R. M., Chin, M., and Ginoux, P.: Global and regional decreases in
2   tropospheric oxidants form photochemical effects of aerosols, J. Geophys. Res., 108, 4097, doi:
3   4010.1029/2002JD002622, 2003.
4   Mauersberger, K., Lämmerzahl, P., and Krankowsky, D.: Stratospheric Ozone Isotope Enrichments—
5   Revisited, Geophys. Res. Lett., 28, 3155-3158, 2001.
6   McCabe, J. R., Boxe, C. S., Colussi, A. J., Hoffmann, M. R., and Thiemens, M. H.: Oxygen isotopic
7   fractionation in the photochemistry of nitrate in water and ice, J. Geophys. Res., 110, D15310, 2005.
8   McCabe, J. R., Savarino, J., Alexander, B., Gong, S., and Thiemens, M. H.: Isotopic constraints on non-
9   photochemical sulfate production in the Arctic winter, Geophys. Res. Lett., 33, L05810,
10   10.1029/2005GL025164, 2006.
11   McCabe, J. R., Thiemens, M. H., and Savarino, J.: A record of ozone variability in South Pole Antarctic
12   snow: Role of nitrate oxygen isotopes, J. Geophys. Res, 112, D12303, doi:10.1029/2006JD007822, 2007.
13   Michalski, G., and Bhattacharya, S. K.: The role of symmetry in the mass independent isotope effect in
14   ozone, Proc. Natl. Acad. Sci., 106, 5493-5496, 2009.
15   Michalski, G., Bhattacharya, S. K., and Girsch, G.: NOx cycle and the tropospheric ozone isotope
16   anomaly: an experimental investigation, Atmos. Chem. Phys, 14, 4935-4953, 10.5194/acp-14-4935-2014,
17   2014.
18   Michalski, G. M., Scott, Z., Kabiling, M., and Thiemens, M. H.: First measurements and modeling of Δ^{17}O
19   in atmospheric nitrate, Geophys. Res. Lett., 30, 1870, doi:1810.1029/2003GL017015, 2003.
20   Morin, S., Savarino, J., Bekki, S., Gong, S., and Bottenheim, J. W.: Signature of Arctic surface ozone
21   depletion events in the isotope anomaly (Δ^{17}O) of atmospheric nitrate, Atmos. Chem. Phys., 6, 6255-
22   6297, 2007.
23   Morin, S., Savarino, J., Frey, M. M., Yan, N., Bekki, S., Bottenheim, J. W., and Martins, J. M. F.: Tracing the
24   Origin and Fate of NO_x in the Arctic Atmosphere Using Stable Isotopes in Nitrate, Science, 322, 730-732,
25   10.1126/science.1161910, 2008.
26   Morin, S., Savarino, J., Frey, M. M., Dominé, F., Jacobi, H.-W., Kaleschke, L., and Martins, J. M. F.:
27   Comprehensive isotopic composition of atmospheric nitrate in the Atlantic Ocean boundary layer from
28   65S to 79N, J. Geophys. Res, 114, D05303, doi:10.1029/2008JD010696, 2009.
29   Morin, S., Sander, R., and Savarino, J.: Simulation of the diurnal variations of the oxygen isotope
30   anomaly (Δ^{17}O) of reactive atmospheric species, Atmos. Chem. Phys, 11, 3653-3671, doi:10.5194/acp-
31   11-3653-2011, 2011.
32   Morton, J., Barnes, J., Schueler, B., and Mauersberger, K.: Laboratory studies of heavy ozone, J. Geophys.
33   Res., 95, 901-907, 1990.
34   Müller, J.-F., Peeters, J., and Stavrakou, T.: Fast photolysis of carbonyl nitrates from isoprene,, Atmos.
35   Chem. Phys, 14, 2497–2508, 10.5194/acp-14-2497-2014, 2014.
36   Murray, L. T., Jacob, D. J., Logan, J. A., Hudman, R. C., and Koshak, W. J.: Optimized regional and
37   interannual variability of lightning in a global chemical transport model constrained by LIS/OTD satellite
38   data, J. Geophys. Res., 117, D20307, 10.1029/2012JD017934, 2012.
39   Murray, L. T.: Lightning NOx and Impacts on Air Quality, Curr. Pollution Rep., 2, 115-133,
40   10.1007/s40726-016-0038-0, 2016.
41   Newsome, B., and Evans, M. J.: Impact of uncertainties in inorganic chemical rate constants on
42   tropospheric ocmposition and ozone radiative forcing, Atmos. Chem. Phys, 17, 14333-14352,
43   10.5194/acp-17-14333-2017, 2017.
44   O'Brien, J., Shepson, P., Muthuramu, K., Hao, C., Niki, H., Hastie, D., Taylor, R., and Roussel, P.:
45   Measurements of alkyl and multifunctional organic nitrates at a rural site in Ontario, J. Geophys. Res.,
46   100, 22795–22804, 1995.

1   Park, R. J., Jacob, D. J., Field, B. D., Yantosca, R. M., and Chin, M.: Natural and transboundary pollution
2   influences on sulfate-nitrate-ammonium aerosols in the United States: implications for policy, J.
3   Geophys. Res., 109, D15204, 10.1029/2003JD004473, 2004.
4   Parrella, J. P., Jacob, D. J., Liang, Q., Zhang, Y., Mickley, L. J., Miller, B., Evans, M. J., Yang, X., Pyle, J. A.,
5   Theys, N., and Roozendael, M. V.: Tropospheric bromine chemistry: implications for present and pre-
6   industrial ozone and mercury, Atmos. Chem. Phys. , 12, 6723-6740, 10.5194/acp-12-6723-2012, 2012.
7   Paulot, F., Crounse, J. D., Kjaergaard, H. G., Kroll, J. H., Seinfeld, J. H., and Wennberg, P. O.: Isoprene
8   photooxidation: new insights into the production of acids and organic nitrates, Atmos. Chem. Phys., 9,
9   1479-1501, 2009.
10   Ramazan, K. A., Syomin, D., and Finlayson-Pitts, B. J.: The photochemical production of HONO during the
11   heterogeneous hydrolysis of NO_2, Phys. Chem. Chem. Phys., 6, 3836-3843, 10.1039/b402195a, 2004.
12   Reed, C., Evans, M. J., Crilley, L. R., Bloss, W. J., Sherwen, T., Read, K. A., Lee, J. D., and Carpenter, L.:
13   Evidence for renoxification in the tropical marine boundary layer, Atmos. Chem. Phys, 17, 4081-4092,
14   10.5194/acp-17-4081-2017, 2017.
15   Richter, A., Borrows, J. P., Nub, H., Granier, C., and Niemier, U.: Increase in tropospheric nitrogen dioxide
16   over China observed from space, Nature, 437, 129–132, 10.1038/nature04092, 2005.
17   Rindelaub, J. D., McAvey, K. M., and Shepson, P. B.: The photochemical production of organic nitrates
18   from α-pinene and loss via acid-dependent particle phase hydrolysis,, A`100tm. Env., 193–201,
19   10.1016/j.atmosenv.2014.11.010, 2015.
20   Romer, P. S., Wooldridge, P. J., Crounse, J. D., Kim, M. J., Wennberg, P. O., Dibb, J. E., Scheuer, E., Blake,
21   D. R., Meinardi, S., Brosius, A. L., Thames, A. B., Miller, D. O., Brune, W. H., Hall, S. R., Ryerson, T. B., and
22   Cohen, R. C.: Constraints on Aerosol Nitrate Photolysis as a Potential Source of HONO and NOx,
23   Environmental Science & Technology, 52, 13738-13746, 10.1021/acs.est.8b03861, 2018.
24   Saiz-Lopez, A., Lamarque, J. F., Kinnison, D. E., Tilmes, S., Ordonez, C., Orlando, J. J., Conley, A. J., Plane,
25   J. M. C., Mahajan, A. S., Sousa Santos, G., ATlas, E. L., Blake, D. R., Sander, S. P., Schauffler, S., Thompson,
26   A. M., and Brasseur, G. P.: Estimating the climate significance of halogen-driven ozone loss in the
27   tropical marine troposphere, Atmos. Chem. Phys, 12, 3939-3949, 10.5194/acp-12-3939-2012, 2012.
28   Savarino, J., and Thiemens, M. H.: Analytical procedure to determine both $\delta^{18}O$ and $\delta^{17}O$ of H_2O_2 in
29   natural water and first measurements, Atmos. Env., 33, 3683-3690, 1999b.
30   Savarino, J., Kaiser, J., Morin, S., Sigman, D. M., and Thiemens, M. H.: Nitrogen and oxygen isotopic
31   constraints on the origin of atmospheric nitrate in coastal Antarctica, Atmos. Chem. Phys., 7, 1925-1945,
32   2007.
33   Savarino, J., Bhattacharya, S. K., Morin, S., Baroni, M., and Doussin, J.-F.: The $NO+O_3$ reaction: A triple
34   oxygen isotope perspective on the reaction dynamics and atmospheric implications for the transfer of
35   the ozone isotope anomaly, J. Chem. Phys., 128, 194303, 10.1063/1.2917581, 2008.
36   Savarino, J., Morin, S., Erbland, J., Grannec, F., Patey, M., Vicars, W., Alexander, B., and Achterberg, E. P.:
37   Isotopic composition of atmospheric nitrate in a tropical marine boundary layer, PNAS, published ahead
38   of print, doi:10.1073/pnas.1216639110, 2013.
39   Schmidt, J. A., Jacob, D. J., Horowitz, H. M., Hu, L., Sherwen, T., Evans, M. J., Liang, Q., Sulieman, R. M.,
40   Oram, D. E., Le Breton, M., Percival, C. J., Wang, S., Dix, B., and Volkamer, R.: Modeling the observed
41   tropospheric BrO background: Importance of multiphase chemistry and implications for ozone, OH, and
42   mercury, J. Geophys. Res., 121, 11,819-811,835, 10.1002/2015JD024229, 2016.
43   Shah, V., Jaeglé, L., Thornton, J. A., Lopez-Hilfiker, F. D., Lee, B. H., Schroder, J. C., Campuzano-Jost, P.,
44   Jimenez, J. L., Guo, H., Sullivan, A. P., Weber, R. J., Green, J. R., Fiddler, M. N., Bililign, S., Campos, T. L.,
45   Stell, M., Weinheimer, A. J., Montzka, D. D., and Brown, S. S.: Chemical feedbacks weaken the
46   wintertime response of particulate sulfate and nitrate to emissions reductions over the eastern United
47   States, Proc. Natl. Acad. Sci., 115, 8110-8115, 10.1073/pnas.1803295115, 2018.

Shao, J., Chen, Q., Wang, Y., Xie, Z., He, P., Sun, Y., Lu, X., Shah, V., Martin, R. V., Philip, S., Song, S., Zhao, Y., Zhang, L., and Alexander, B.: Heterogeneous sulfate aerosol formation mechanisms during wintertime Chinese haze events: Air quality model assessment using observations of sulfate oxygen isotopes in Beijing, Atmos. Chem. Phys, 19, 6107-6123, 10.5194/acp-19-6107-2019, 2019.

Sharma, H. D., Jervis, R. E., and Wing, K. Y.: Isotopic exchange reactions in nitrogen oxides, J. Phys. Chem., 74, 923-933, 1970.

Sherwen, T., Schmidt, J. A., Evans, M. J., Carpenter, L. J., Brobmann, K., Eastham, S. D., Jacob, D. J., Dix, B., Koenig, T. K., Sinreich, R., Ortega, I. K., Volkamer, R., Saiz-Lopez, A., Prados-Roman, C., Mahajan, A. S., and Ordonez, C.: Global impacts of tropospheric halogens (Cl, Br, I) on oxidants and composition in GEOS-Chem, Atmos. Chem. Phys, 16, 12239-12271, 10.5194/acp-16-12239-2016, 2016.

Sherwen, T., Evans, M. J., Sommariva, R., Hollis, L. D. J., Ball, S. M., Monks, P. S., Reed, C., Carpenter, L. J., Lee, J. D., Forster, G., Bandy, B., Reeves, C. E., and Bloss, W. J.: Effects of halogens on European air-quality, Faraday Discuss., 200, 75-100, 10.1039/C7FD00026J, 2017.

Singh, H. B., Herlth, D., O'Hara, D., Zahnle, K., Bradshaw, J. D., Sandholm, S. T., Talbot, R., Crutzen, P. J., and Kanakidou, M.: Relationship of Peroxyacetyl nitrate to active and total odd nitrogen at northern high latitudes: Influence of reservoir species on NO_x and O_3, J. Geophys. Res, 97, 16,523-516,530, 1992.

Sofen, E. D., Alexander, B., Steig, E. J., Thiemens, M. H., Kunasek, S. A., Amos, H. M., Schauer, A. J., Hastings, M. G., Bautista, J., Jackson, T. L., Vogel, L. E., McConnell, J. R., Pasteris, D. R., and Saltzman, E. S.: WAIS Divide ice core suggests sustained changes in the atmospheric formation pathways of sulfate and nitrate since the 19th century in the extratropical Southern Hemisphere, Atmos. Chem. Phys. , 14, 5749-5769, 10.5194/acp-14-5749-2014, 2014.

Spataro, F., and Ianniello, A.: Sources of atmospheric nitrous acid: State of the science, current research needs, and future prospects, Journal of the Air and Waste Management Association, 64, 1232-1250, 10.1080/10962247.2014.952846, 2014.

Stettler, M. E. J., Eastham, S., and Barrett, S. R. H.: Air quality and public health impacts of UK airports. Part I: Emissions, Atm. Env., 45, 5415-5424, 10.1016/j.atmosenv.2011.07.012, 2011.

Tan, F., Tong, S., Jing, B., Hou, S., Liu, Q., Li, K., Zhang, Y., and Ge, M.: Heterogeneous reactions of NO_2 with $CaCO_3$–$(NH_4)_2SO_4$ mixtures at different relative humidities, Atmos. Chem. Phys, 16, 8081-8093, 10.5194/acp-16-8081-2016, 2016.

Thiemens, M. H., T. Jackson: Pressure dependency for heavy isotope enhancement in ozone formation, Geophys. Res. Lett., 17, 717-719, 1990.

Tong, S. R., Hou, S. Q., Zhang, Y., Chu, B. W., Liu, Y. C., He, H., Zhao, P. S., and Ge, M. F.: Exploring the nitrous acid (HONO) formation mechanism in winter Beijing: direct emissions and heterogeneous production in urban and suburban areas, Faraday Discuss., 189, 213-230, 10.1039/c5fd00163c, 2016.

Vicars, W., and Savarino, J.: Quantitative constraints on the [17]O-excess ($\Delta^{17}O$) signature of surface ozone: Ambient measurements from 50°N to 50°S using the nitrite-coated filter technique, Geochem. Cosmochem. Acta, 135, 270-287, 10.1016/j.gca.2014.03.023, 2014.

Vicars, W. C., Bhattacharya, S. K., Erbland, J., and Savarino, J.: Measurement of the 17O-excess ($\Delta^{17}O$) of tropospheric ozone using a nitrite-coated filter, Rapid Commun. Mass Spectrom., 26, 1219-1231, 10.1002/rcm.6218, 2012.

Vinken, G. C. M., Boersma, K. F., Jacob, D. J., and Meijer, E. W.: Accounting for non-linear chemistry of ship plumes in the GEOS-Chem global chemistry transport model, Atmos. Chem. Phys, 11, 11707-11722, 10.5194/acp-11-11707-2011, 2011.

von Glasow, R., and Crutzen, P. J.: Model study of multiphase DMS oxidation with a focus on halogens, Atmos. Chem. Phys., 4, 589-608, 2004.

Wang, F., Michalski, G., Seo, J., and Ge, W.: Geochemical, isotopic, and mineralogical constraints on atmospheric deposition in the hyper-arid Atacama Desert, Chile, Geochem. Cosmochem. Acta, 135, 29-48, 10.1016/j.gca.2014.03.017, 2014.

1   Wang, J. Q., Zhang, X. S., Guo, J., Wang, Z. W., and Zhang, M. G.: Observation of nitrous acid (HONO) in
2   Beijing, China: Seasonal variation, nocturnal formation and daytime budget, Science of the Total
3   Environment, 587, 10.1016/j.scitotenv.2017.02.159, 2017.
4   Wang, X., Jacob, D. J., Eastham, S., Sulprizio, M., Zhu, L., Chen, Q., Alexander, B., Sherwen, T., Evans, M.
5   J., Lee, B. H., Haskins, J., Lopez-Hilfiker, F. D., Thornton, J. A., Huey, L. G., and Liao, H.: The role of
6   chlorine in tropospheric chemistry, Atmos. Chem. Phys. Discuss., 10.5194/acp-2018-1088, 2018.
7   Wang, Y. H., Jacob, D. J., and Logan, J. A.: Global simulation of tropospheric O_3-NO_x hydrocarbon
8   chemistry 1. Model formulation, J. Geophys. Res., 103, 10,713-710,725, 1998.
9   Xu, L., Guo, H., Boyd, C. M., Klein, M., Bougiatioti, A., Cerully, K. M., Hite, J. R., Isaacman-VanWertz, G.,
10 Kreisberg, N. M., Knote, C., Olson, K., Koss, A., Goldstein, A. H., Hering, S. V., de Gouw, J., Baumann, K.,
11 Lee, S.-H., Nenes, A., Weber, R. J., and Ng, N. L.: Effects of anthropogenic emissions on aerosol formation
12 from isoprene and monoterpenes in the southeastern United States, Proc. Natl. Acad. Sci., 112, 37–42,
13 10.1073/pnas.1417609112, 2015.
14 Xu, W., Kuang, Y., Zhao, C., Tao, J., Zhao, G., Bian, Y., Yu, Y., Shen, C., Liang, L., and Zhang, G.: NH3-
15 promoted hydrolysis of NO2 induces explosive 1 growth in HONO, Atmos. Chem. Phys. Discuss.,
16 https://doi.org/10.5194/acp-2018-996, 2018.
17 Yabushita, A., Enami, S., Sakamoto, Y., Kawasaki, M., Hoffman, M. R., and Colussi, A. J.: Anion-Catalyzed
18 Dissolution of NO2 on Aqueous Microdroplets, J. Phys. Chem. A Lett., 113, 4844–4848,
19 10.1021/jp900685f, 2009.
20 Yang, X., Cox, R. A., Warwick, N. J., Pyle, J. A., Carver, G. C., O'Connor, F. M., and Savage, N. H.:
21 Tropospheric bromine chemistry and its impact on ozone: A model study, J. Geophys. Res, 110, D2331,
22 doi:10.1029/2005JD003244, 2005.
23 Ye, C., Zhou, X., Pu, D., Stutz, J., Festa, J., Spolaor, M., Tsai, C., Cantrell, C., Mauldin Iii, R. L., Campos, T.,
24 Weinheimer, A., Hornbrook, R. S., Apel, E., Guenther, A., Kaser, L., Yuan, B., Karl, T., Haggerty, J., Hall, S.,
25 Ullmann, K., Smith, J. N., Ortega, J., and Knote, C.: Rapid cycling of reactive nitrogen in the marine
26 boundary layer, Nature, 532, 489-491, 10.1038/nature17195, 2016.
27 Ye, C., Zhou, X., Pu, D., Stutz, J., Festa, J., Spolaor, M., Tsai, C., Cantrell, C., Mauldin III, R. L., Weinheimer,
28 A., Hornbrook, R. S., Apel, E. C., Guenther, A., Kaser, L., Yuan, B., Karl, T., Haggerty, J., Hall, S., Ullmann,
29 K., Smith, J., and Ortega, J.: Tropospheric HONO distribution and chemistry in the southeastern US,
30 Atmos. Chem. Phys, 18, 9107-9120, 10.5194/acp-18-9107-2018, 2018.
31 Zare, A., Romer, P. S., Nguyen, T., Keutsch, F. N., Skog, K., and Cohen, R. C.: A comprehensive organic
32 nitrate chemistry: insights into the lifetime of atmospheric organic nitrates, Atmos. Chem. Phys.
33 Discuss., 10.5194/acp-2018-530, 2018.
34 Zhang, L., Gong, S., Padro, J., and Barrie, L.: A size-segregated particle dry deposition scheme for an
35 atmospheric aerosol module, Atmos. Env., 35, 549-560, 2001.

39

40

41

1 **Table 1.** Calculated $\Delta^{17}O$(nitrate) in the model for each nitrate production pathway (X = Br, Cl,
2 and I; HC = hydrocarbon; MTN = monoterpene; ISOP = isoprene; $\Delta^{17}O(O_3^*) = 39‰$). A is
3 defined in equation E1.

	Nitrate formation pathway	Δ^{17}**O(nitrate)**
	Gas-phase reactions	
R1	$NO_2 + OH$	$\frac{2}{3}A\Delta^{17}O(O_3^*)$
R2	$NO_3 + HC$	$(\frac{2}{3}A + \frac{1}{3})\Delta^{17}O(O_3^*)$
R3	$NO + HO_2$	$\frac{1}{3}A\Delta^{17}O(O_3^*)$
	Aerosol uptake from the gas-phase followed by hydrolysis	
R4	$N_2O_5 + H_2O_{(aq)}$	$(\frac{2}{3}A + \frac{1}{6})\Delta^{17}O(O_3^*)$
R5	$N_2O_5 + Cl^-_{(aq)}$	$(\frac{2}{3}A + \frac{1}{3})\Delta^{17}O(O_3^*)$
R6	$XNO_3 + H_2O_{(aq)}$	$(\frac{2}{3}A + \frac{1}{3})\Delta^{17}O(O_3^*)$
R7	$NO_2 + H_2O_{(aq)}$	$\frac{2}{3}A\Delta^{17}O(O_3^*)$
R8	$NO_3 + H_2O_{(aq)}$	$(\frac{2}{3}A + \frac{1}{3})\Delta^{17}O(O_3^*)$
R9	$RONO_2 + H_2O_{(aq)}$ (where $RONO_2$ is from $NO + RO_2$)	$\frac{1}{3}A\Delta^{17}O(O_3^*)$
R10	$RONO_2 + H_2O_{(aq)}$ (where $RONO_2$ is from $NO_3 + MTN/ISOP$)	$(\frac{2}{3}A + \frac{1}{3})\Delta^{17}O(O_3^*)$
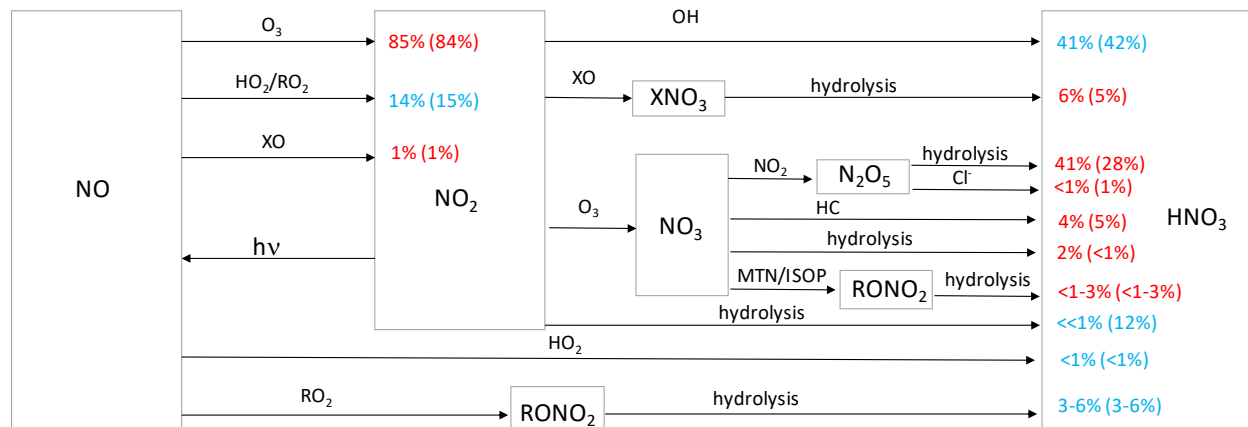
3   **Figure 1.** Simplified HNO_3 formation in the model. Numbers show the global, annual mean percent
4   contribution to NO_2 and HNO_3 formation in the troposphere below 1 km for the "cloud chem"
5   ("standard") simulation. Red indicates reactions leading to high $\Delta^{17}O$ values, blue indicates reactions
6   leading to low $\Delta^{17}O$ values. $HO_2 = HO_2+RO_2$; X = Br+Cl+I; HC = hydrocarbons; MTN = monoterpenes;
7   ISOP = isoprene.
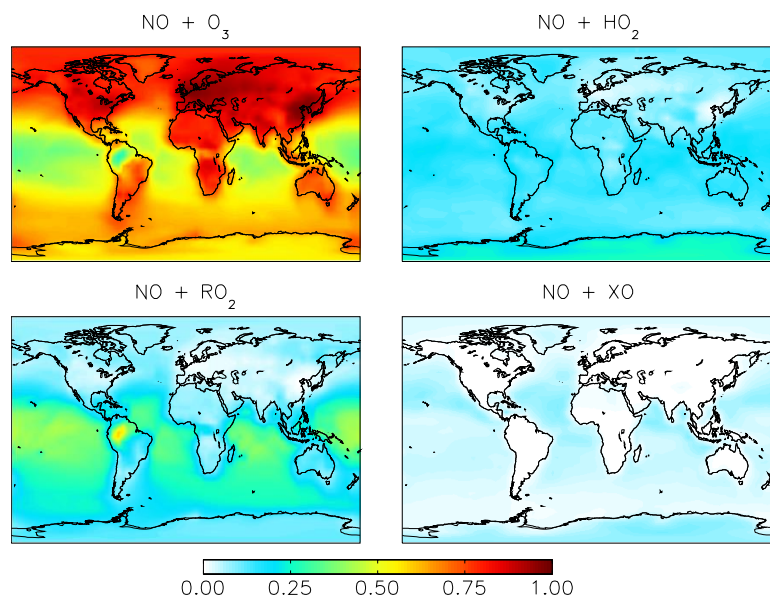
11   **Figure 2.** Annual-mean fraction of NO_2 formation from the oxidation of NO in the troposphere below 1
12   km altitude in the "cloud chemistry" model.

Figure 3. Annual-mean fraction of HNO₃ formation from the oxidation of NO_x in the troposphere below 1 km altitude in the "cloud chemistry" model.
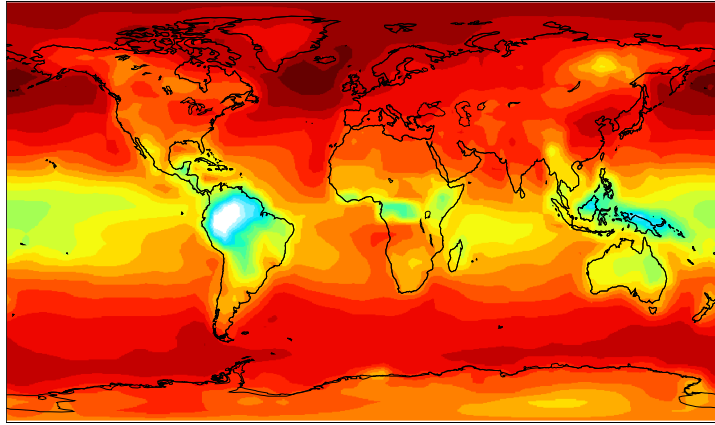
3   **Figure 4.** Modeled, annual-mean Δ^{17}O(nitrate) below 1 km altitude for the "cloud chemistry" model.
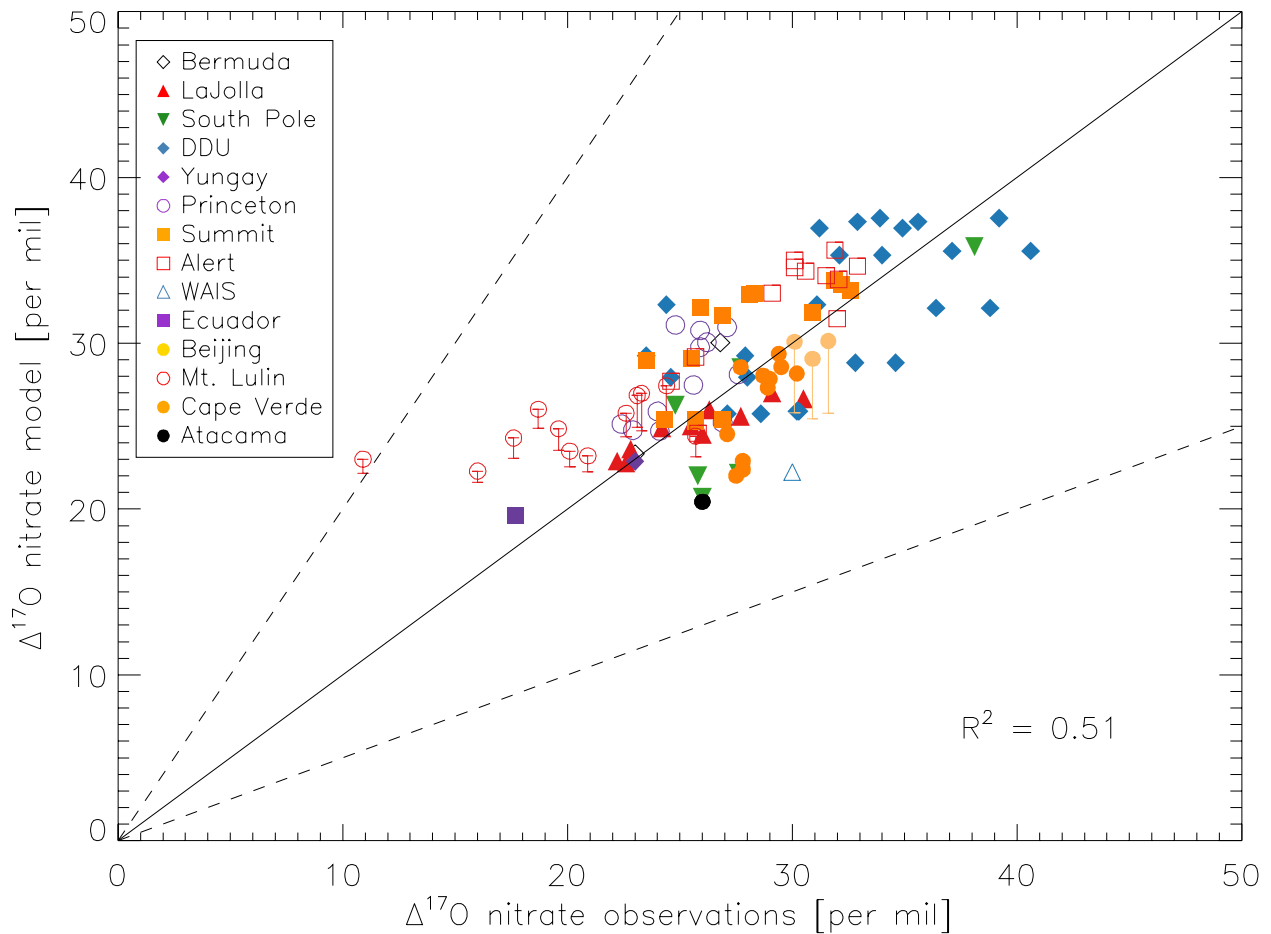
Figure 5. Comparison of monthly-mean modeled ("cloud chemistry") and observed Δ^{17}O(nitrate) at
locations where there are enough observations to calculate a monthly mean. References for the
observations are in the text. The error bars represent different assumptions for calculated modeled A
values for nighttime reactions as described in the text. Error bars for Beijing and Mt. Lulin reflect the
range of possible modeled A values for nighttime reactions as described in the text. The y=x (solid line)
and y = 2x and y = 0.5x (dashed) are shown.
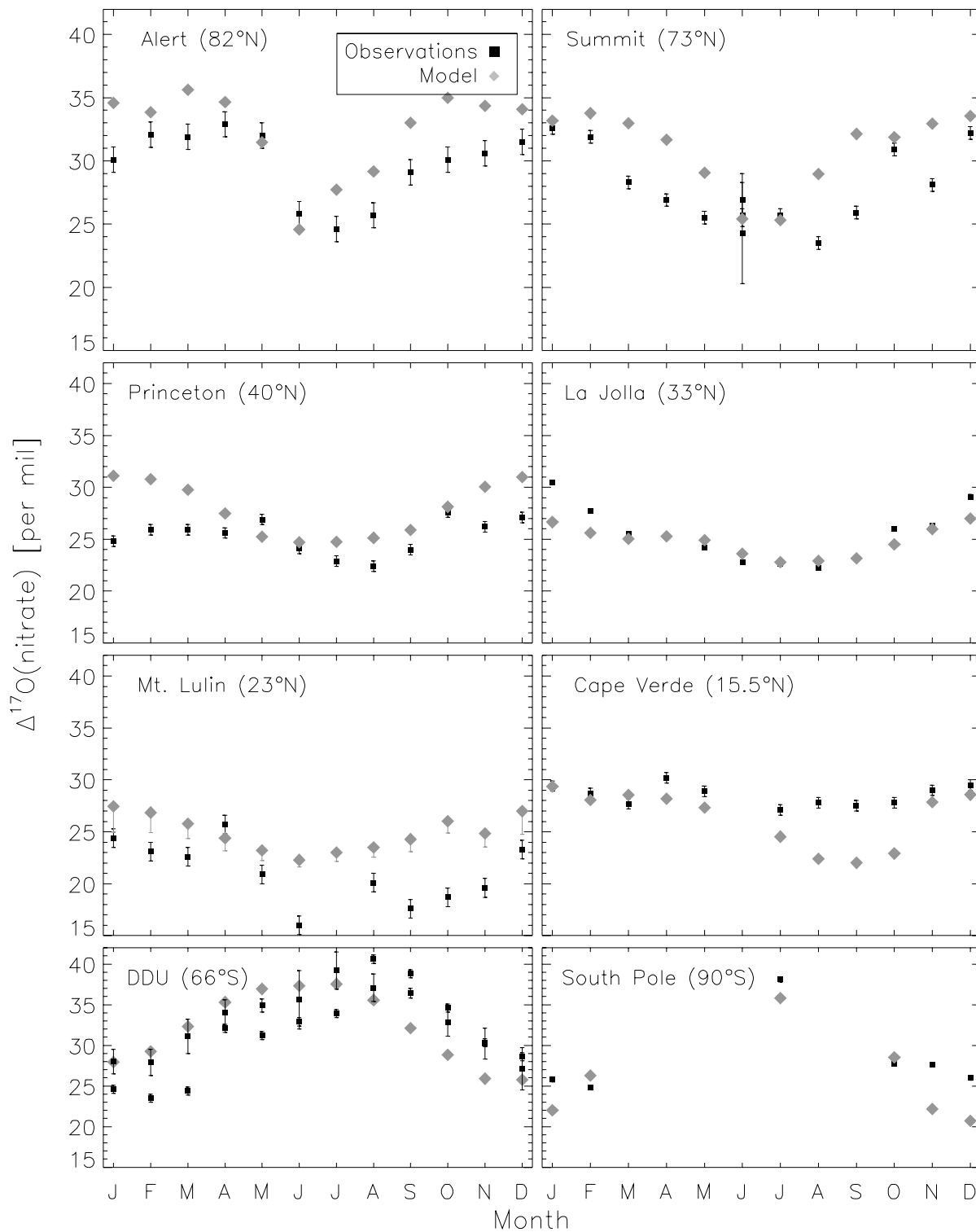
Figure 6. Comparison of monthly-mean modeled ("cloud chemistry") and observed $\Delta^{17}O$(nitrate). Error bars for model results from Mt. Lulin reflect the range of possible modeled *A* values for nighttime reactions as described in the text. Error bars for the observations reflect the analytical uncertainty in the measurements, except for two data points in June for Summit which reflect the standard deviation of $\Delta^{17}O$(nitrate) from multiple measurements during that month.
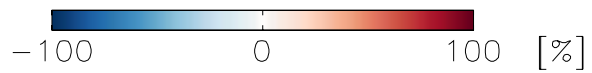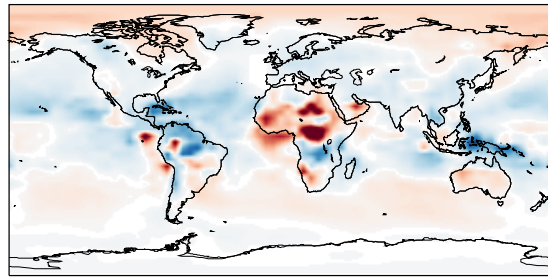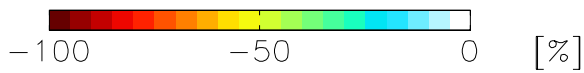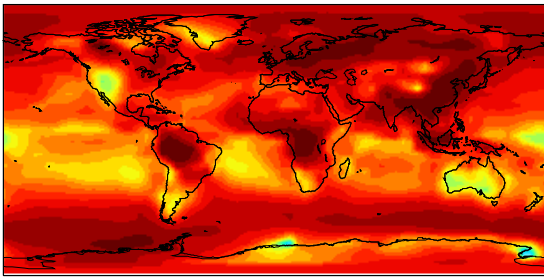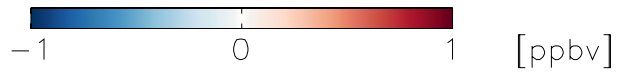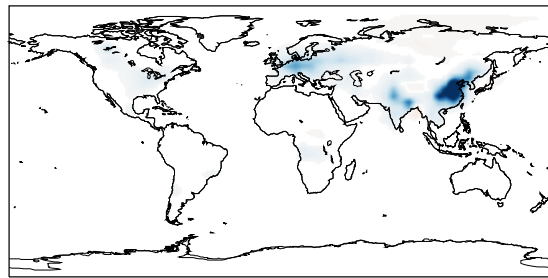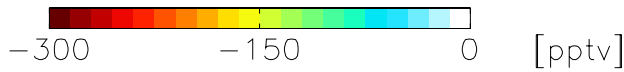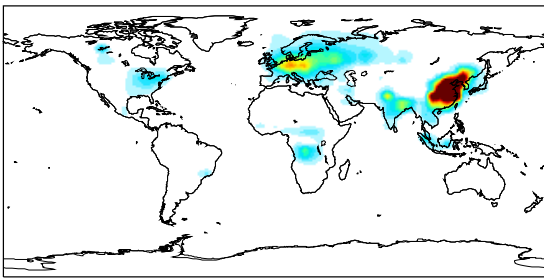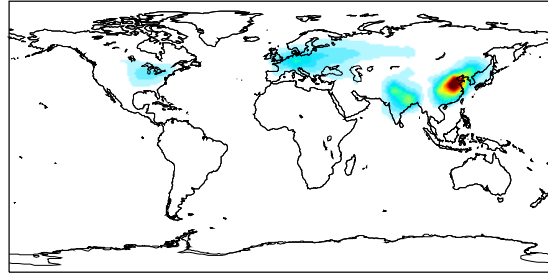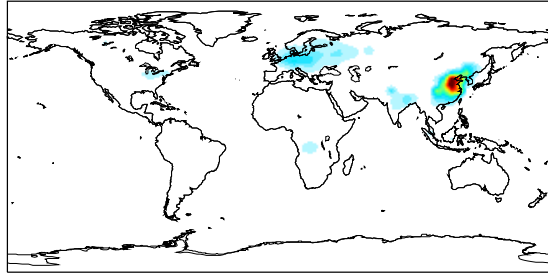
Figure 7. Modeled annual-mean HONO (left) and fine-mode nitrate (right) concentrations below 1 km altitude in the "standard" simulation (top) with $\gamma_{NO2} = 10^{-4}$ for NO_2 hydrolysis. Absolute (middle) and relative (bottom) change in concentrations below 1 km altitude between the "standard" model and the model simulation with $\gamma_{NO2} = 10^{-7}$. Negative numbers represent a decrease relative to the standard simulation.
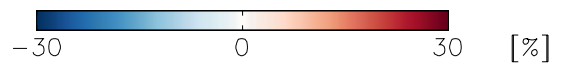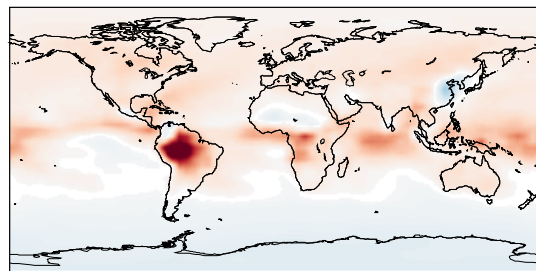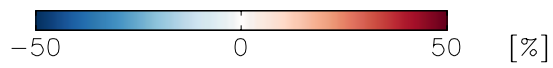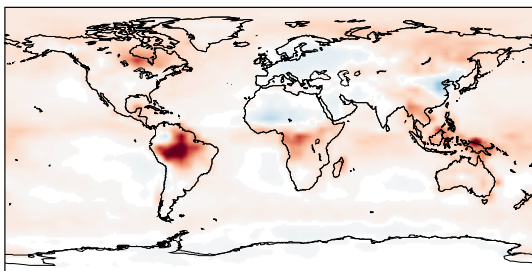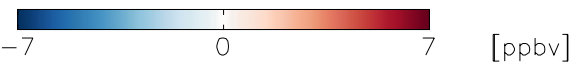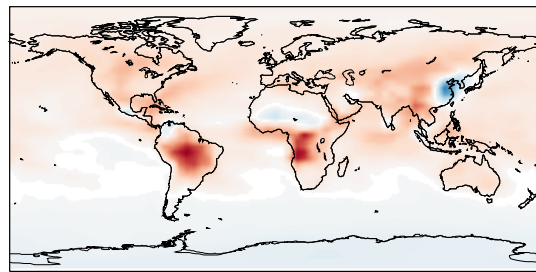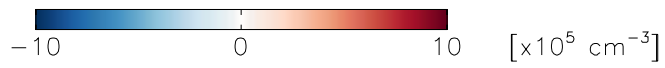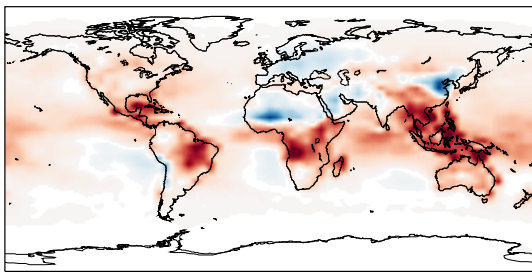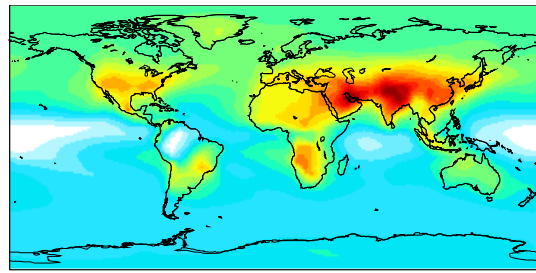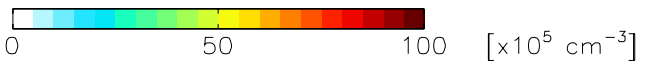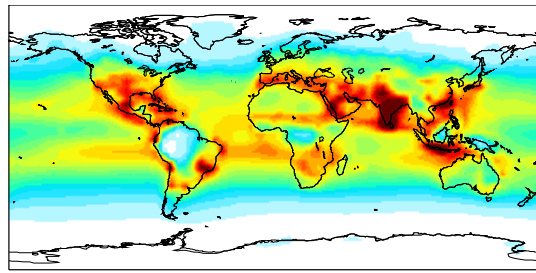
Figure 8. Same as Figure 7 except for OH (left) and ozone (right).
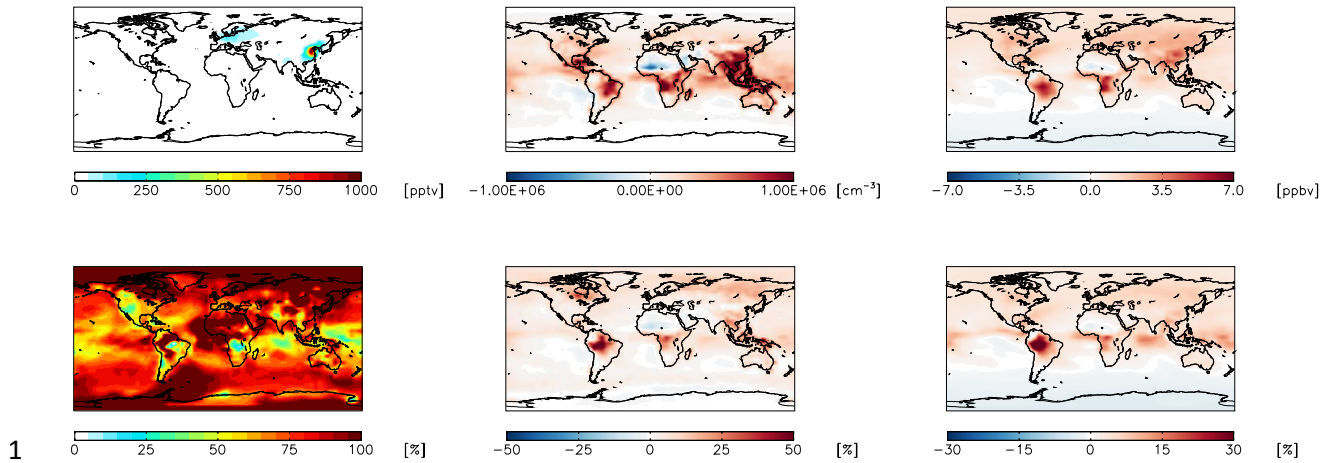
Figure 9. Absolute (top) and relative (bottom) change in HONO (left), OH (middle), and ozone (right) concentrations below 1 km altitude between the "standard" model and the model simulation with an acidity-dependent yield from NO_2 hydrolysis. Positive numbers represent an increase relative to the "standard" simulation.
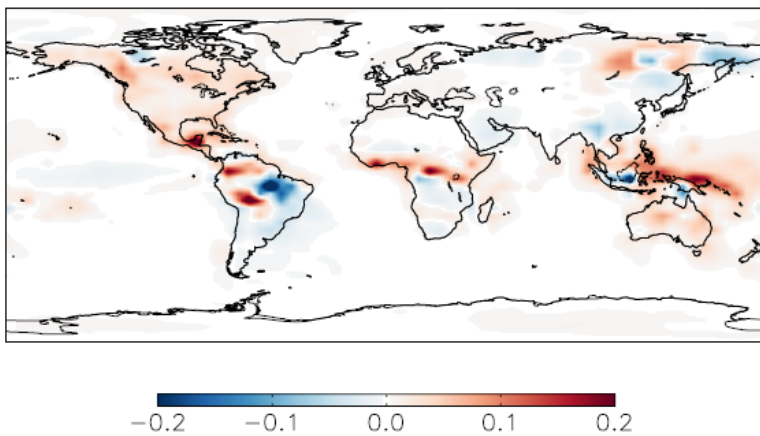
Figure 10. Modeled annual-mean difference in the fractional production rate of HNO_3 from the hydrolysis of organic nitrate below 1 km attitude in the year 2015 relative to 2000 (2015 – 2000).